Efficient planar heterojunction based on α-sexithiophene/fullerene through the use of MoO3/CuI anode buffer layer

H. Ftouhi, E.M. El-Menyawy, H. Lamkaouane, M. Diani, G. Louarn, J.C. Bernède, M. Addou, L. Cattin

Efficient Planar Heterojunction Based on α-Sexithiophene/Fullerene through the use of MoO_3/CuI Anode Buffer Layer

H. Ftouhi [1,2]*, E.M. El-Menyawy [2,5], H. Lamkaouane [2,4], M. Diani [1], G. Louarn[2], J.C. Bernède [3], M. Addou [1], L. Cattin [2]

[1] Équipe de Recherche Couches Minces et Nanomatériaux – Faculté des Sciences et Techniques, Université Abdelmalek Essaâdi, BP 416, Tanger – Maroc

[2] Université de Nantes, Institut des Matériaux Jean Rouxel (IMN), CNRS, UMR 6502, 2 rue de la Houssinière, BP 92208, 44000 Nantes, France

[3] Université de Nantes, MOLTECH-Anjou, CNRS, UMR 6200, 2 rue de la Houssinière, BP 92208, 44000 Nantes, France

[4] Laboratory of Physics of Condensed Matter and Renewable Energy, Faculty of Sciences and Technology, Hassan II University of Casablanca B.P 146, Mohammedia, Morocco

[5] Solid-State Electronics Laboratory, Solid-State Physics Department, Physics Research Division, National Research Centre, 33 El-Bohouth St., Dokki, Giza 12622, Egypt

Abstract

In this work, planar heterojunction organic photovoltaic cells (PHJ-OPVs) based on alpha-sexithiophene (α-6T) and fullerene active materials were investigated. We have studied the effect of the hole transporting layer (HTL) on the performances of the PHJ-OPVs. The studied HTLs are molybdenum trioxide (MoO_3), MoO_3 coupled cuprous iodide (MoO_3/CuI) and CuI. The PHJ-OPVs were fabricated using thermal evaporation/sublimation technique. The experimental study shows that the double HTL MoO_3/CuI using 1.5 nm of CuI thickness improves significantly the efficiency of the PHJ-OPVs compared with those with single HTLs. This enhancement is due to the fact that MoO_3 participate to the optimization of the holes collection and CuI causes significant influence on the nucleation and the growth of α-6T. CuI has led to spectacular modification, in the structural properties of α-6T. When α-6T deposited onto ITO/MoO_3, the α-6T layers are amorphous, while they are crystallized into monoclinic crystalline structure with a laying down molecular orientation when deposited onto ITO/MoO_3/CuI. The use of the double HTL and the optimization of the α-6T deposition parameters have led to an important improvement in the α-6T light absorption, roughness and the holes mobility. These findings participate to the significant enhancement of the PHJ-OPVs performances and their life time.

Keywords: Organic photovoltaic cells; Hole transporting layer; Hybrid buffer layer; Molybdenum trioxide; Cuprous iodide; α-Sexithiophene/Fullerene

1. Introduction

Due to demographic growth and economic expansion, the increase in global energy consumption is not about to slow down. Forecasts show that by 2035 this increase will be up to 40% [1]. Given their limited reserves and their participation in greenhouse gas emissions, the contribution of fossil fuels, which is currently dominant, must in the near future give way to renewable energies [1] [2]. Among these, solar energy is the most abundant on earth. One of the examples to make the most of this free energy is photovoltaic effect, which is the basic principle used in photovoltaic solar cells. Organic photovoltaics cells (OPVs), provide a unique opportunity as a next-generation photovoltaic technology due to their lightness, flexibility, low cost [3], environmental-friendly, semi-transparency and easy to be integrated into existing infrastructure [1] [4], also, they are visually pleasing.

Today, OPVs see a remarkable increase in their performances, due to the synthesis of more efficient materials and optimized OPVs configurations. The active layer of OPVs is based on a couple electron donor/electron acceptor (ED/EA). Depending of the ED/EA interface, two mains architectures were developed, either bulk heterojunction (BHJ), which consists in a blend ED/EA, or planar heterojunction (PHJ), which consists in stacked ED/EA layers. In recent years, significant improvements in the efficiency of BHJ-OPVs were achieved through the synthesis of polymerous material donors and no-fullerene electron acceptors with advanced chemical and physical properties [5] [6]. Nevertheless, if it is desirable to increase the OPV efficiency, other parameters should not be overlooked such as yield of chemical synthesis, simple OPVs grow process, performance reproducibility. Thereby, substituting a polymer by small molecule, which exhibits inherent mono-dispersity and well-defined structure, allows obtaining more reproducible results. In the same way, small molecules allow to achieve easily planar heterojunction organic solar cells (PHJ-OPVs), through successive sublimations, which purify the deposited molecules. Moreover, PHJ configuration simplifies the interface geometry, which permits to study more easily the chemical and physical interactions between the stacked layers [7]

In the last few years oligothiophene family, α-sexithiophene (α-6T) in particular, has gotten much attention for different applications such as organic field effect transistors, light emitting diodes [8] [9] [10] and as donor material in organic solar cells because of its high hole mobility [11], reasonable absorbance in the visible range, high purity, simple synthesis and easy chemical modification by changing the number of thiophene rings [3] [12]. Actually, the maximum power conversion efficiency (PCE) of 8.4% was achieved using three-layer PHJ device structure, where, α-6T was the principle donor material [13].

The process of selecting the donor material, should be done carefully, to ensure a good absorption and exciton diffusion efficiencies. Moreover, in order to obtain high carrier collection efficiency, it is necessary to insert a hole transporting layer (HTL) and an electron transporting layer at the interfaces organic active

layers/anode and cathode respectively. The HTL allows improving hole collection efficiency via the adjustment of the band matching at the interface ED/anode [14] [15]. Beyond this effect on the adjustment of the band structure, the HTL may also influence the growth of the organic layer superimposed on it. Thus it can modify the orientation of the molecules constituting the ED layer and therefore its properties [14]. Π-conjugated molecules, such as α-6T, have highly anisotropic properties, such as carrier mobility and light absorption, which depend on the molecular orientation [16] [17] [18].

On one hand, the investigations have demonstrated that Molybdenum trioxide (MoO_3) is an efficient material as HTL because it leads to a significant enhancement in the PV parameters by enhancing the band matching between the work function of the anode and the Highest Occupied Molecular Orbital (HOMO) of the donor materials [19]. However, no significant changes have taken place on the structural and the morphological properties of π-conjugated molecules by using MoO_3 as HTL [19].

On the other hand, it was demonstrated that the control of the molecular orientation of the π-conjugated molecules can be achieved by different techniques: thermal annealing, vapor annealing, optical heating under laser beam irradiation [20], keeping the films overnight (12 h) under vacuum [21] or using specific under-layer. For instance, some studies have shown that an ultra-thin copper iodide (CuI) film can be used to control the molecular orientation of the π-conjugated molecules [22]. Moreover, J-C. Bernède et al. have demonstrated that a double anode buffer (ABL) layer of MoO_3/CuI leads to a very interesting enhancement in the PCE of 2.50% by using thienylenevinylene–triphenylamine with peripheral dicyanovinylene groups (TDCV–TPA) as ED [14]. Such a hybrid layer allows to add to the optimization of the holes collection thanks to MoO_3, the improvement of the morphology of the organic layer due to the presence of CuI. In the same way, it was demonstrated that CuI enhances the absorbance of different Metal Phthalocyanines, such as CuPc, ZnPc and PbPc, used as EDs in OPVs by changing the molecular orientation to a specific molecular order [23] [24] [25] [26].

Bilayer PHJs-OPVs based on the α-6T/fullerene (C_{60}) couple were previously reported in the literature, but in the most cases the HTL used was PEDOT:PSS(Poly(3,4-ethylenedioxythiophene)-poly(styrenesulfonate) [27] [28] [13], which is known by its highly hygroscopic and acidic properties which has detrimental effects on the lifetime of the device [29] [48]. So, the objective of this study was the investigation of α-6T/C_{60} PHJ-OPVs system using free-PEDOT:PSS HTL. We studied the effect of different HTLs : MoO_3, CuI and MoO_3/CuI on the performances of α-6T/C_{60} PHJ-OPVs system. We demonstrated that the use of thinner film of CuI coupled with MoO_3 layer changes the α-6T structure from amorphous to crystalline phase. Therefore, we observed an important enhancement on the absorbance of α-6T film and its roughness. These findings beside the optimization of the deposition parameters of the α-6T layer are the reasons to obtain an important enhancement in the efficiency and the life time of α-6T/C_{60} system by the use of MoO_3/CuI HTL.

2. Experimental details

2.1. Materials and methods

Our device thin films were fabricated using vacuum sublimation technique. The substrates are glass (25mm x 25mm) coated Indium Tin Oxide (ITO), where the ITO is the anode material of a sheet resistance of ~15 Ω/sq and a thickness of 100 nm. 30% of the ITO surface layer was etched, cleaned, heated up at 80°C and then loaded into the vacuum chamber (10^{-4} Pa). The chemical products used to grow the HTL layers are molybdenum trioxide (MoO_3, 99.99%) and copper(I) iodide (CuI, 98%) powders. The donor material source was the sublimed α-6T, its chemical formula is $C_{24}H_{14}S$. The acceptor material used is the Buckminster fullerene (C_{60}, 99.9%). The C_{60} powder was deposited by sublimation using a speed rate of 0.06-0.08 nm/s. The donor, acceptor chemical structures are displayed in the **Fig. 1.a**. The material used to grow the exciton blocking layer was Tris-(8-hydroxyquinoline) Aluminum (Alq_3, 99.9 %), its chemical formula is $C_{27}H_{18}AlN_3O_3$. It was also deposited by sublimation by the use of a very slow speed rate of 0.01-0.03 nm/s. The source of the cathode reflexive material was aluminum (Al) wires. The counter electrode was deposited by sublimation in a cross-bar architecture; with an active device area of about 0.1 cm^2.

The studied stacked device architecture was: Glass/ITO (100 nm)/HTL/ α-6T (x nm)/C_{60} (45 nm)/Alq_3 (9 nm)/Al (100 nm) (**Fig. 1.b**). The HTLs used were : MoO_3(4 nm), MoO_3(4 nm)/CuI(y nm) and CuI(1.5 nm) but the study will be mainly focused in details on the effect of MoO_3 and MoO_3/CuI HTLs on the PV performances of the PHJ-OPVs. All the layers thicknesses outlined here and their deposition speed rate have been already optimized in some previous studies of our team [31], except α-6T, which thickness has been varied from x =18 nm to 24 nm in order to determine its optimum value. The deposition speed rate of the α-6T layer was also optimized during the study. With regard to the hybrid HTL layer, previous studies have shown that MoO_3 thickness is not critical, similar results are obtained when its thickness varies from 3 nm to 5 nm. About the CuI layer, its thickness and, mainly, its deposition rate are more decisive. When deposited too fast, its surface roughness is very high, which induces leakage currents. Therefore it is necessary to use a very slow deposition rate, 0.005 nm s^{-1} [32].

As described in the reference [33] the work functions values (W_F) of ITO, MoO_3 and CuI were estimated using a Kelvin Probe instrument. The measured values were $W_{F\text{-}ITO}$ = 4.7 eV, $W_{F\text{-}MoO3}$ =5.3 eV and $W_{F\text{-}CuI}$ = 5.2 eV. The energy diagram of our device is represented in the **Fig. 1.c**. This figure shows that α-6T has a HOMO (Highest Occupied Molecular Orbital) of 5.3 eV while the C_{60} LUMO (Lowest Unoccupied Molecular Orbital) is 4.4 eV. The theoretical open circuit voltage (V_{oc}) is determined by the energy difference between HOMO of the donor and the LUMO of the acceptor following the Equation 1. In our heterojunction the maximum theoretical V_{oc} is 0.9 eV.

$$eV_{oc} = \left(E_{HOMO_D} - E_{LUMO_A}\right) - \Delta \qquad \textbf{Eq. 1}$$

where, Δ is linked to the excitons binding energy, radiative and non-radiative losses.

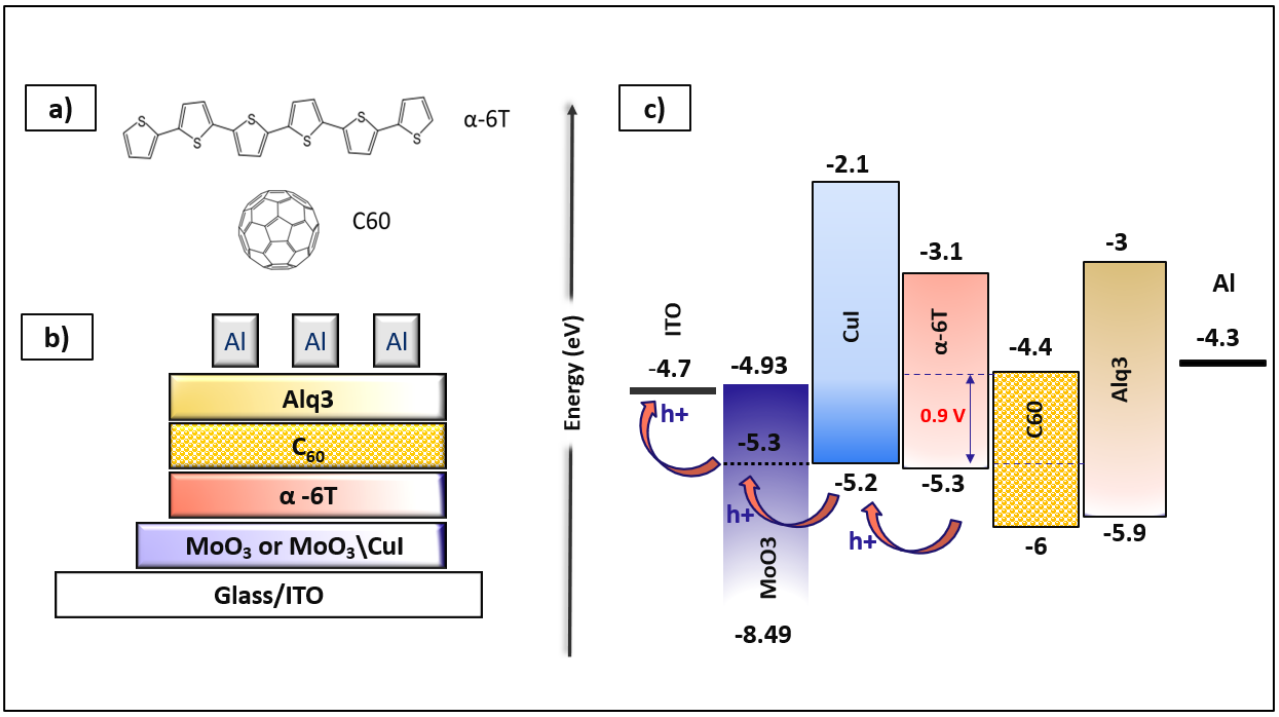

Fig.1. Chemical structures of the active materials(a), stacked device architecture (b) and a representation of the energy diagram of the studied system (c).

2.2. Characterization techniques

The prepared organic solar cells were characterized in dark and under illumination at an intensity of 100 mW/cm^2. The illumination source is a xenon lamp with an AM1.5G using a LOT-Oriel 300 W solar simulator. The measurements have been taken in the direct polarization and the cells have been illuminated through the ITO electrode. All the current-voltage measurements were carried out in the ambient conditions. The average OPVs performances, at least 18 samples were probed over three runs, as six diodes were realized for each run.

In order to check the influence of the HTLs on the hole mobility of α-6T we proceeded to carrier mobility measurement using the space charge limited current (SCLC) method. 'Hole only' devices were as follow: ITO/MoO_3 (4 nm)/ α-6T (60 nm)/MoO_3 (7 nm)/Al. The organic films probed were thick of 80 nm because it must be thick enough to prevent that interface phenomena dominate those of bulk.

For the optical characterizations, the spectra were recorded using a Carry spectrophotometer with a step of 1 nm in the wavelength range of 330–600 nm. The structural properties of the α-6T thin films were investigated by using X-Ray Diffractometer Bruker D8 A25 « Da Vinci » system, equipped with a Cu anode tube and second generation Si strip detector ("LynxEye XE"), with Cu Kα radiation (λ = 1.5418 Å),

this device has θ/θ geometry. The morphological properties were investigated using the scanning electron microscopy (SEM) JEOL JSM 7600F equipped with a Schottky Field Emission Gun and a system of electron detectors placed in the lens, the operating voltage used is 5kV. In order to identify precisely the roughness of the samples in the following, we have used Nikon Eclipse Atomic Force Microscope (AFM) and we have utilized Antimony Si n-doped tip in tapping mode ("Centre de micro-characterization, Institut des Matériaux Jean Rouxel, Université de Nantes").

3. Results and discussion

3.1. Optimization of the HTL material

We have started by the preparation of two series of PHJ-OPVs based α-6T/ C_{60} active layers using the following structure : ITO (100 nm)/HTL/α-6T (20 nm)/C_{60}(45 nm)/Alq_3(9 nm)/Al (100 nm). The studied parameter was the HTL layer. We have used two different HTLs : MoO_3 (4 nm) and MoO_3 (4 nm)/CuI (1.5 nm). Both series have been prepared using a standard thickness of α-6T 20 nm. Usually, this thickness value is used to start the optimization of a donor material thickness and we will focus in the section 3.2.2 to its optimization. The current density *vs*. voltage characteristics (J-V) of the devices are presented in the **Fig. 2** and the characteristic parameters are summarized in the **Table 1**. By comparing the performances of both prepared solar cells with and without CuI(1.5nm), it is clearly seen from the **Fig. 2** and the **Table. 1**, that the insertion of CuI leads to an important increase of the open circuit voltage (V_{oc}) by 0.15V, the short circuit current density (J_{sc}) by 1.86 mA/cm^2 and the fill factor (FF) by 6%, which directly enhances the PCE of the cell from 0.74% to 1.74%.

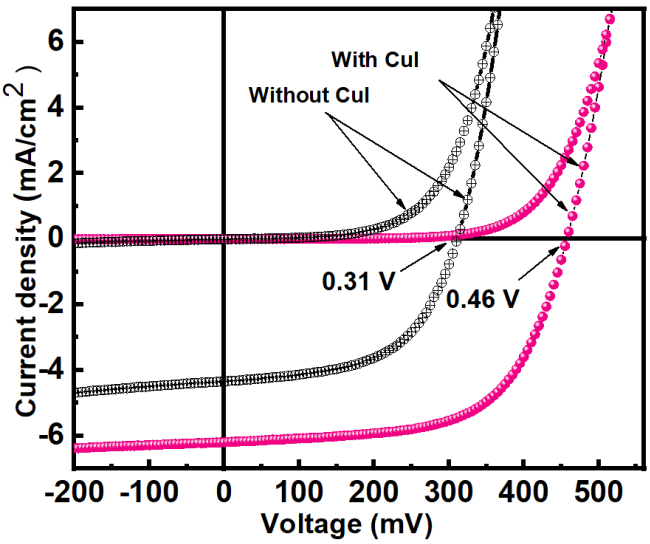

Fig. 2. Electrical OPV devices characteristics with MoO_3/CuI(1.5 nm) (●) and MoO_3 (⊕) HTLs

In order to check more precisely the influence of the CuI layer on the OPVs performances, we have increased the thickness of CuI to 3 nm in the hybrid HTL, and then we have prepared cells with CuI(1.5 nm) as HTL but without MoO_3 layer. The obtained PV parameters of these cells are presented in **Table 1**. The increase in the CuI thickness to 3 nm leads to an important decrease in the FF. This behavior can be

attributed to the increase in the surface roughness of CuI due to the increase in its thickness such surface roughness increase induces an increase of the leakage current of the OPVs and therefore a decrease of FF. The same behavior was observed in the study done by *M. Makha et al [49].*

Also, the growth of the cell system using CuI alone as HTL leads to a decrease in the PV performances comparing with the cell prepared with MoO_3/CuI(1.5nm). The FF decreases from 61% to 44%, the short J_{sc} from 6.19 to 5.80 mA/cm^2 and the V_{oc} from 0.46 to 0.41V. This behavior has led to a decrease in the PCE from 1.74% to 1.06%. These results can be explained by the increase in the leakage currents due to the absence of MoO_3. The same behavior was observed earlier in the references [24] and [49].

Table 1. Variation of the PV parameters of PHJ-OPVs with the HTL used : MoO_3 or MoO_3/CuI(1.5 nm), MoO_3/CuI(3 nm) and CuI(1.5 nm)

HTL	α-6T thickness (nm)	CuI thickness (nm)	V_{oc} (V)	J_{sc} (mA/cm^2)	FF (%)	PCE (%)
MoO_3	20	----	0.31 ± 0.04	4.33 ± 0.50	55 ± 3	0.74 ± 0.30
MoO_3/CuI	20	1.5	0.46 ± 0.03	6.19 ± 0.40	61 ± 3	1.74 ± 0.25
MoO_3/CuI	20	3	0.41 ± 0.05	5.99 ± 0.50	54 ± 4	1.33 ± 0.35
CuI	20	1.5	0.41 ±0 .05	5.80 ± 0.60	44 ± 5	1.06 ± 0.40

3.2.Optimization of the performances of the α-6T/C_{60} devices

After showing that the MoO_3/CuI(1.5 nm) is the best HTL, and because of the dependence of the PV parameters to the thickness and the deposition speed rate of the ED, we need to optimize the deposition parameters of α-6T. We have used different speed rates; 0.03-0.04 nm/s (slow), 0.04-0.06 nm/s (medium) and 0.06-0.08 nm/s (fast) and different thicknesses: 18, 22 and 24 nm. These parameters have been controlled in-situ through the use of a calibrated quartz microbalance.

3.2.1. Optimization of the deposition speed rate

As can be seen from the **Fig. 3**, all the samples with different speed rates exhibit a rod-like texture with a uniform rods distributed on the whole scanned surface. From the preliminary observations we can notice that there is no significant modification on the α-6T morphological properties, but if we focus on the inset images with higher magnifications, we can observe that the growth of α-6T using the medium deposition speed rate quite increases the α-6T diameters rods, their interconnections and intercalations.

Fig.4. represents the optical density of the MoO_3/CuI(1.5 nm)/α-6T samples deposited using different speed rates. The α-6T deposited with a medium speed rate participates to a small enhancement of the absorption spectrum of the α-6T by increasing the absorption by 3.5% in the range of [400-520 nm] and a slight widening of the spectrum towards the red region. These features can enhance the photons harvesting. This

observed red broadening may be explained by the small increase in the α-6T rods interconnections observed in the SEM images using the medium speed rate of 0.04-0.06 nm/s.

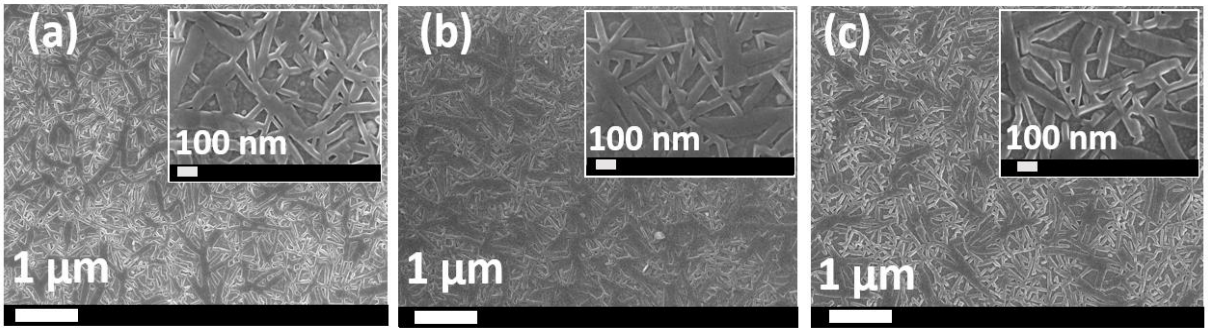

Fig. 3. SEM images of the α-6T deposited with different speed rates (a) low speed (0.01-0.03 nm/s), (b) medium speed rate (0.04 – 0.06 nm/s) and fast speed rate (0.06-0.08 nm/s). Inset. larger magnification.

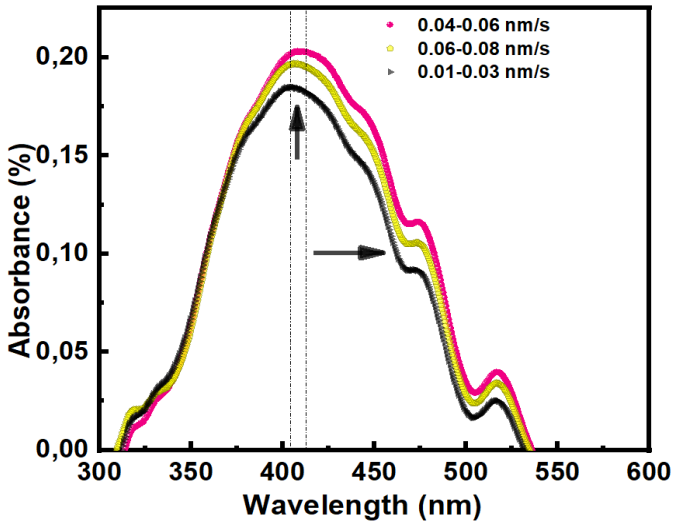

Fig. 4. Optical density spectrums of α-6T films deposited with low speed (0.01-0.03 nm/s), medium speed rate (0.04 – 0.06 nm/s) and fast speed rate (0.06-0.08 nm/s).

3.2.2. Optimization of the α-6T thickness

Then we have studied the influence of α-6T layer thickness on the performance of the PHJ-OPVs: ITO/MoO_3/CuI/α-6T(x)/C_{60}/Alq_3/Al with x = 18, 22, and 24 nm. The obtained results are summarized in Table 2. As it was expected, the OPVs parameters are influenced by increasing the α-6T thickness from 18 nm to 24 nm. We have observed an increase in the V_{oc} and J_{sc} when the thickness increases up to 22 nm. However, by making α-6T thicker to 24 nm, V_{oc} and J_{sc} decrease. Whereas, we can notice that the FF decreases with the increase of the α-6T thickness. This may be explained by the increase of the excitons recombination due to the increase in the series resistance by increasing the thickness of the donor material because of the small diffusion lengths of excitons in organic semiconductors limit the thickness which is

further limited by the low charge carrier mobility [34]. Then we have proceeded to some specific characterizations to understand why the MoO_3/CuI(1.5 nm) HTL causes such enhancement in the PV parameters of the OPVs comparing with the cell with MoO_3 alone. We have deposited α-6T thin film on MoO_3 and on MoO_3/CuI(1.5 nm), and we have done structural, optical and morphological analyses.

Table 2. Variation of the PV parameters of the α-6T/C_{60} OPVs with α-6T thickness and the PV parameters of the cell prepared with the optimum α-6T thickness using MoO_3 HTL alone.

HTL	α-6T thickness (nm)	V_{oc} (V)	J_{sc} (mA/cm^2)	FF (%)	PCE (%)
MoO_3/CuI(1.5 nm)	18	0.43 ± 0.04	3.40 ± 0.50	63 ± 4	0.93 ± 0.30
	20	0.46 ± 0.03	6.19 ± 0.40	61 ± 3	1.74 ± 0.25
	22	**0.50 ± 0.03**	**6.10 ± 0.35**	**58 ± 4**	**1.77 ± 0.25**
	24	0.46 ± 0.03	5.44 ± 0.45	55 ± 5	1.38 ± 0.30
MoO_3	**22**	**0.31± 0.04**	**4.25 ± 0.5**	**56 ± 3**	**0.74 ± 0.30**

Fig. 5. represents the X-ray diffractograms of the both samples. The ITO/MoO_3/α-6T sample shows that the α-6T layer is amorphous. While, α-6T film deposited on ITO/MoO_3/CuI(1.5 nm), shows a polycrystalline monoclinic structure as testified by the apparition of diffraction peaks. The peak situated at 2θ = **20°** stems from the $(11\bar{2})$ lattice plan of the high temperature α-6T polymorph, and the other peak represents the (020) plane of the low temperature polymorph. The (020) and $(11\bar{2})$ peaks indicate a lying-down molecular orientation [21].

Fig. 6 represents the absorption spectra of α-6T deposited on MoO_3 and MoO_3/CuI(1.5 nm). The onset of the absorption is situated at 340 nm. It is quite clear that the CuI enhances strongly the absorption of the α-6T film. The maximum broad absorption appears at 405.6 nm (3.05 eV), it is attributed to aggregates in the film, whereas the other peaks at 476 nm and 516 nm are due to the isolated α-6T molecules [35].

The change noticed in the α-6T color from nearly transparent in the case when it is deposited on MoO_3, to yellow when it is deposited on MoO_3/CuI(1.5 nm) reveals a birefringence property (images inserted in the **Fig. 6**). This optical behavior, also confirms the lying down molecular orientation of the molecules when they are deposited on CuI. The same behavior was observed by Mizokuro et al. [36] when they have deposited α-6T on polythiophene polymer (PT).

For the α-6T deposited on ITO/CuI(1.5 nm) alone, we have obtained the same crystalline phase structure but the intensities of the peaks were lower than ITO/MoO_3/CuI(1.5nm)/α-6T sample. Also, the same absorption features were obtained in the case of α-6T deposited on ITO/CuI(1.5 nm) but the absorption was weaker by comparing with the film deposited on the double HTL. The XRD diffractograms and the

absorption spectra of the ITO/CuI/α-6T are presented in the supporting information Figures S1 and S2 respectively. These results justify the low performances obtained when CuI is used alone.

In order to investigate the effect of CuI on the surface morphology of the α-6T, we have analyzed the samples by SEM. The corresponding images are displayed in the **Fig. 7**. α-6T deposited on MoO_3 alone exhibits a continuous film surface, with apparition of some aggregates on the top of the surface, which increases the roughness of the film (**Fig. 7a**). While, when α-6T is deposited on MoO_3/CuI, its surface has a continuous rod-like texture (**Fig. 7b**). The rods are distributed randomly on the CuI surface with different diameters in the average of 30 nm.

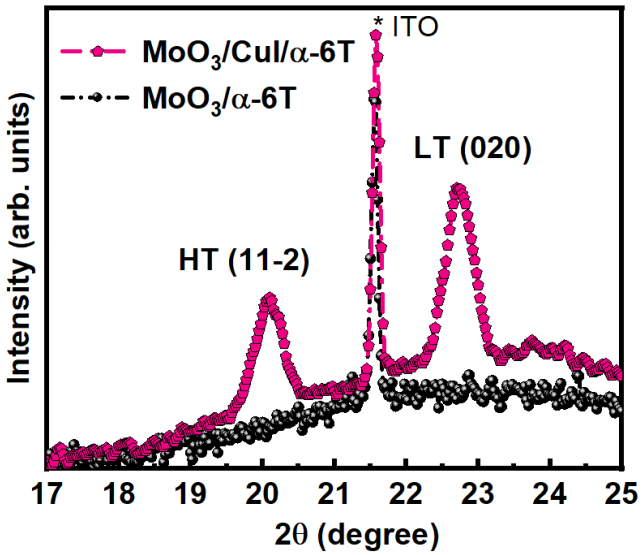

Fig. 5. XRD patterns of α-6T films deposited on ITO/MoO_3 and ITO/MoO_3/CuI(1.5 nm)

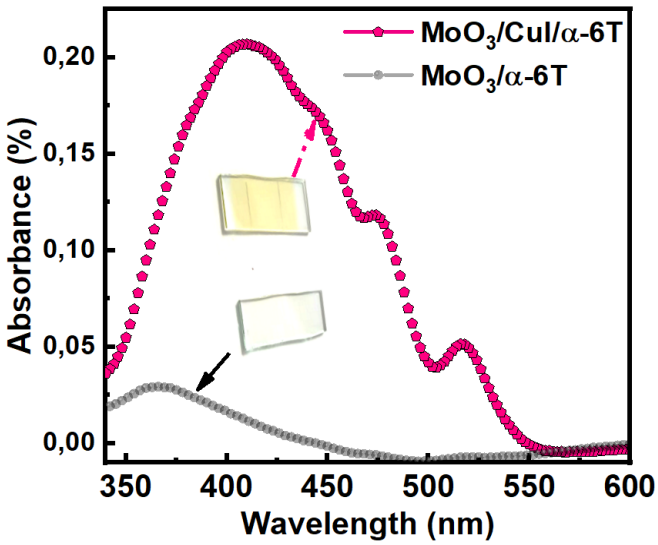

Fig. 6. Optical density spectrums of α-6T films deposited on ITO/MoO_3 and ITO/MoO_3/CuI(1.5 nm)

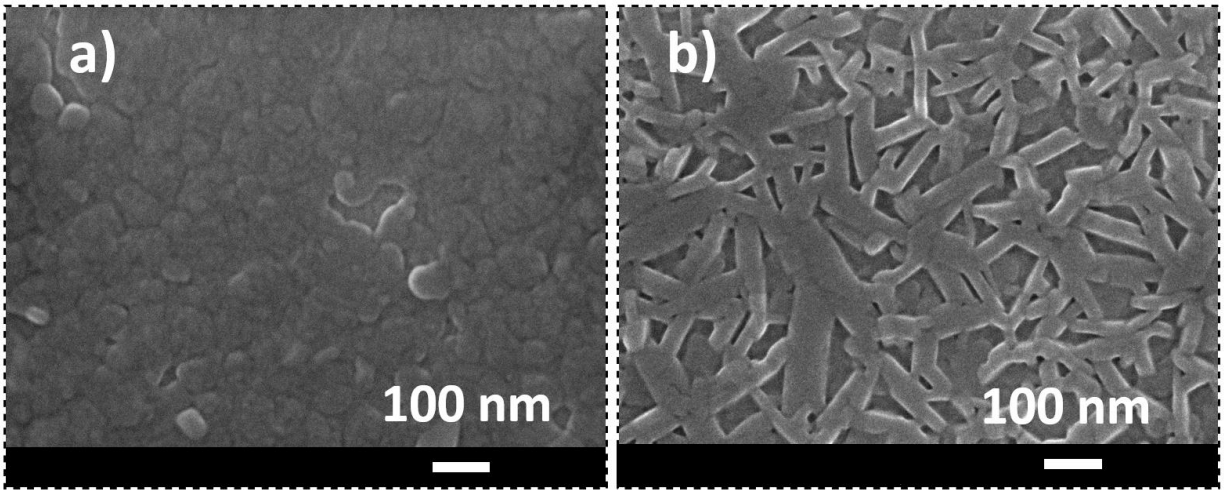

Fig.7. SEM images of the α-6T deposited on MoO_3 (a) and on MoO_3/CuI (1.5 nm)(b)

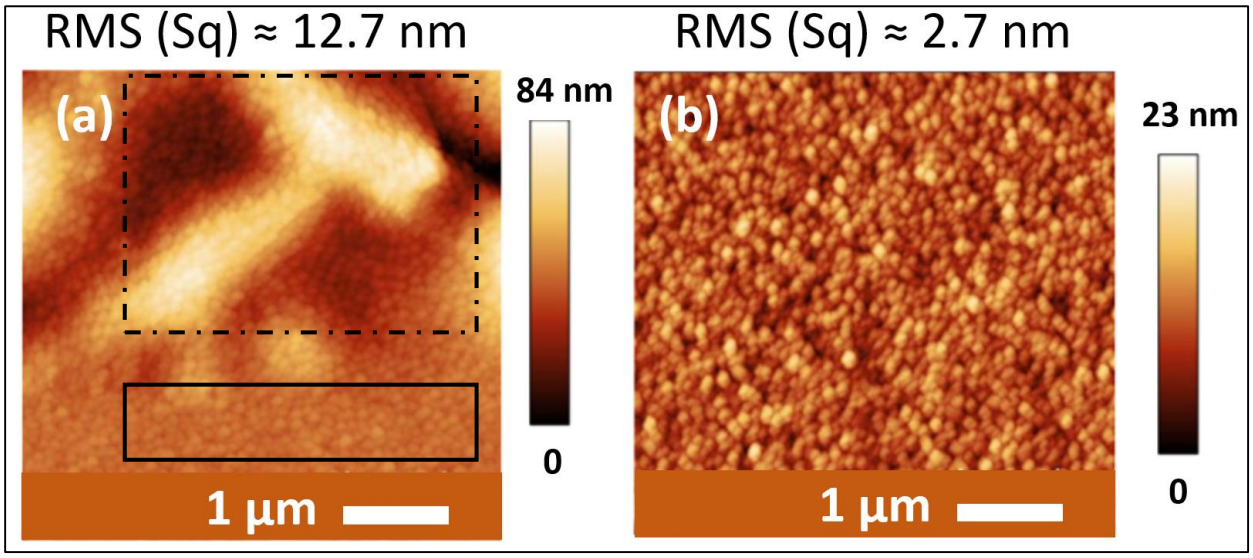

Fig.8. AFM images of the α-6T deposited on MoO_3 (a) and on MoO_3/CuI(1.5 nm) (b)

The roughness of the samples has been deduced from the images obtained by the means of the AFM. The images presented in the **Fig. 8**. MoO_3/α-6T sample exhibits two regions with different topographies (**Fig. 8a**). In the upper region (*marked by discontinuous dashes*) appears some knolls and valleys with an average roughness of about RMS =12.7 nm, while the region below (indicated by continuous dashes) is continuous with small grains, its Root Mean Square (RMS) roughness is of about 1.9 nm. Whereas, MoO_3/CuI(1.5 nm)/α-6T shows a homogenous distribution of small grains with an average RMS of about 2.7 nm (**Fig. 8b**). The increase in the surface roughness of α-6T when deposited on MoO_3 increases the area of organic-organic heterojunction , this induces to an important recombination loss [27], which explains the V_{oc} drop observed in the cell with MoO_3 alone.

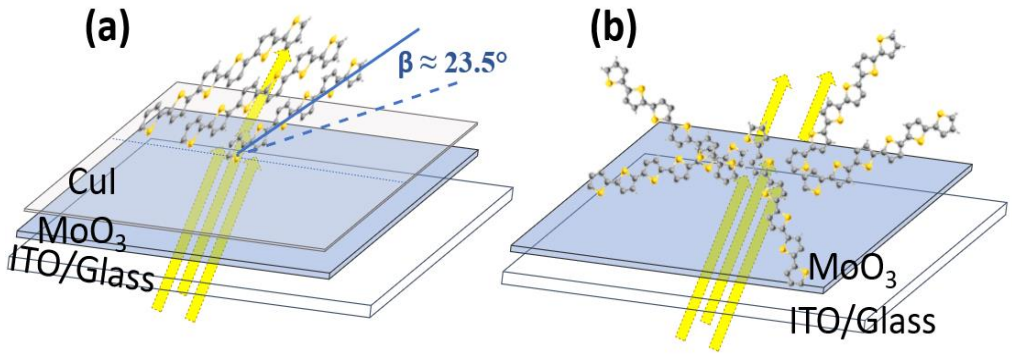

Fig.9. Schematic illustration of the absorption dependence of the α-6T in the case of ordered structure with the laying down molecular orientation (ITO/MoO_3/CuI/α-6T) (a) and the disordered structure (ITO/MoO_3/α-6T) (b)

3.2.3. Specific characterizations of the α-6T layer deposited on MoO_3 or MoO_3/CuI(1.5 nm).

In order to check the influence of the HTL on the hole mobility of α-6T we proceeded to carrier mobility measurement using the space charge limited current (SCLC) method. 'Hole only' devices were as follow: ITO/HTL/α-6T (60 nm)/MoO_3(7 nm)/Al. The organic films probed were thick of 60 nm because it must be thick enough to prevent that interface phenomena dominate those of bulk.

In the SCLC regime, if we suppose uniform charge-carrier mobility, the J–V curve follows the Mott–Gurney law [37]:

$$J = \frac{9}{8}\varepsilon_r\varepsilon_0\mu_h\frac{V^2}{L^3} \qquad \textbf{Eq :2}$$

with ε_0 the vacuum permittivity, ε_r the dielectric constant, μ_h the hole mobility, V the voltage, and L is the thickness of the organic layer. As estimated from SCLC measurements, the hole mobility of polycrystalline α-6T films, i.e., films deposited on MoO_3/CuI(1.5 nm), is $2.5 \cdot 10^{-3} cm^2V^{-1}s^{-1}$, in the case of amorphous films, i.e., films deposited on MoO_3, it is only $1.2 \cdot 10^{-3} cm^2V^{-1}s^{-1}$, which means that it is equal to half of that deposited on MoO_3/CuI(1.5 nm). The same enhancement was observed in the mobility of tris(dicyanovinyl–triphenylamine) TDCV–TPA by using MoO_3/CuI as the HTL [14] [38].

3.3. Discussion

As shown above, the effect of CuI on the device performances is very significative. The observed increase of the short current density by using MoO_3/CuI(1.5 nm) can be explained theoretically by the complimentary advantages between MoO_3 and CuI. MoO_3 allows adjusting the energy barrier between the anode work function, which is 4.7eV for the cleaned ITO, and the HOMO of the α-6T (5.3 eV), while the iodine atoms of CuI are good electron acceptors, by consequence, the holes density and their mobility may increase in the valence band. Which can explain the observed enhancement of the J_{sc} (Table 2) [39].

From the XRD results **Fig. 5**, the radical change of α-6T layers structure from amorphous (disordered orientation) to a crystalline structure with the lying down molecular orientation by the introduction of CuI(1.5 nm), maximizes the electron transition probability because of the quasi-parallel direction between $\pi - \pi^*$ of the α-6T molecules and the electric vector of light [40]. As it was estimated from SCLC measurement, the holes mobility of α-6T increases via the introduction of CuI this observed behavior corroborate with the literature, that the laying down molecular orientation is favorable to increase the holes mobility and their transport [28] [21]. Moreover, the higher mobility allows to increase the conductivity of the α-6T films which can explain the observed small increase in the fill factor of the OPVs cells with MoO_3/CuI(1.5nm) HTL [33]. **Fig. 6.** shows a spectacular enhancement in the absorption of α-6T by introducing MoO_3/CuI HTL because of the obtained lying down molecular orientation. This is due to the fact that the direction of the transition dipole moment is along the long molecular axis. So, in the case of α-6T deposited on MoO_3 alone, it is amorphous, thus, the optical absorption is very weak. These findings confirm the highly anisotropic properties in the light absorption of α-6T [16] as it is explained by the schematic illustration presented in the **Fig. 9.** These absorption results corroborate with the X-ray diffractograms to explain the enhancement observed in the J_{sc} in the cell with MoO_3/CuI(1.5nm).

Moreover, we have obtained an important improvement of the V_{oc} from 0.31V to 0.50 V after addition of CuI(1.5 nm) layer. The V_{oc} is generally related to the effective energy gap following the equation 1, but it hinges on a number of parameters, such as the exciton generation rate, the recombination rate, the carrier mobility and the defect density in the donor material. So, the observed enhancement of the V_{oc} in the cells with MoO_3/CuI HTL, can be explained by the obtained crystalline structure of α-6T, because the crystalline conjugated molecules are very advantageous for donor material as the crystalline state contributes to the increase of the open circuit voltage due to the reduction of the defect density [41], and also, as said above, the increase in the holes mobility of α-6T increases conductivity, by consequence, the recombination mechanisms can be reduced as described by Langevin theory [42]. Moreover, Duhm et al. has shown that a change from vertical to horizontal orientations of α-6T increases its ionization potential energy (IP) by ≈ 0.4 eV due to the modified surface dipole [43], which agrees with our results. Therefore, we assume that the increase in IP originates from the horizontal orientations of α-6T, thus the Voc increases in our case.

In the same context and from the morphological investigations, the decrease of the average roughness from 12.7 nm to 2.7 nm, via the addition of CuI(1.5 nm) layer, encourages the excitons diffusion to reach the interface D/A [27]. Consequently, these reasons explain the increase in the short current density, the open circuit voltage and the fill factor for the OPVs using the hybrid HTL, which results in a PCE of 1.77%. By comparing our results with those obtained by Cnops et al.[13] using the same donor and acceptor while the HTL was PEDOT:PSS, our results show an enhancement in the V_{oc}, J_{sc} and FF by 0.08V, 1.54 mA/cm^2 and 3.4% respectively. Consequently, our device shows an increase of the PCE by 58%. This may be due to the double effect of our HTL; MoO_3 is a good hole's extractor and CuI leads to an increase in the photon harvesting of the active layer due to its potential to crystalize the α-6T layer. From a different angle, our

results are in good agreement with those of Taima et al. who have also demonstrated that the use of CuI on PEDOT:PSS in a PHJ-OPVs based α-6T/SubPc (Boron-substituted Phthalcyanine Choloride) active layers increases the PCE from 1.19 % to 1.77%, by keeping the films overnight in vacuum [21].

In order to go far in the interpretation of the effect of MoO_3/CuI(1.5 nm) HTL on the device performances, we have used the J-V curves to estimate the saturation current, (J_{sat}), J_{sat} being estimated from the curve J_{ph}= f (V_{eff}). Here, the photocurrent density J_{ph} corresponds to the difference between J_L, the current density under $AM_{1.5}$ in light and J_D is the current density in dark and V_{eff}, the effective voltage, is defined by the difference between the voltage V_0 at the open circuit conditions, i.e., for J_{ph} = 0, and the applied bias voltage V_a. In Fig. 10, the curves J_{ph} vs V_{eff} show that the saturation states are achieved at V_{eff} of about 1 V. The J_{sat} values deduced from these curves are presented in **Table 3**. From these values it is possible to estimate the maximum exciton generation rate, G_{max}, and the exciton dissociation probability [P(E,T)] using the following formulas [44] [45].

$$G_{max} = \frac{J_{sat}}{q.L} \qquad \textbf{Eq :3}$$

$$P(E,T) = \frac{J_{ph}}{J_{sat}} \qquad \textbf{Eq :4}$$

Where L is the thickness of the active layers and q is the elemental electric charge.

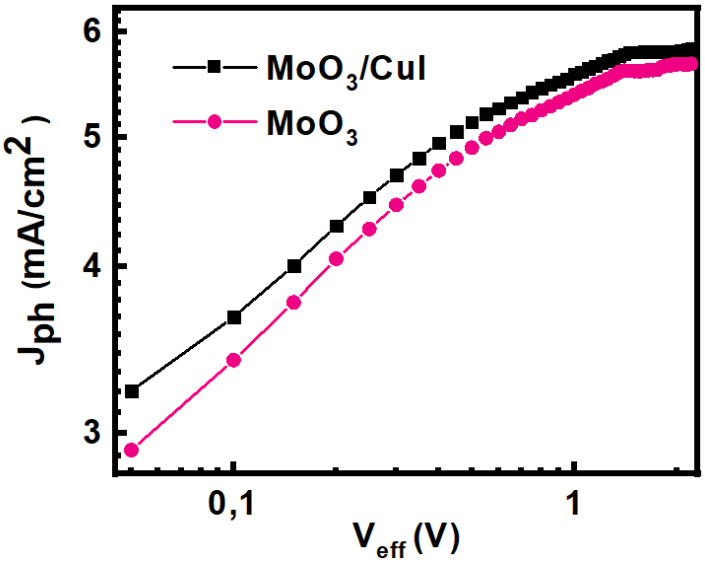

Fig. 10. J_{ph} vs. V_{eff} curves for α-6T/C_{60}PHJ-OPVs with the both HTL: MoO_3 and MoO_3/CuI(1.5 nm).

From the Fig. 10, we can observe that the saturation state is reached at about a V_{eff} of 1.6 V for the both OPVs. It can be seen in Table 3 that there is an increase of the saturation photocurrent density, J_{sat}, by ~21% in the OPV with MoO_3/CuI(1.5 nm).

Consequently, the estimated maximum exciton generation rate, G_{max}, increases. This G_{max} increase suggests an increase of the global exciton generation. This may be due to the influence produced by the hybrid HTL on the structural and the optical properties of α-6T. The calculated value of the exciton dissociation

probability, P(E,T), at short circuit conditions for the devices, gives an estimation of the efficiency of charge separation and collection. We have obtained an increase of the P(E,T) with the use the double HTL MoO_3/CuI(1.5 nm), indicating a higher charge collection efficiency in this device. This may be explained by the less bimolecular recombination activity in these OPVs.

Table 3. Different physical parameters estimated from the J_{ph} vs. V_{eff} curves for the PHJ-OPVs with and without CuI(1.5 nm).

	J_{sat}(mA/cm^2)	J_{ph}(mA/cm^2)	G_{max} (Photon/m^3.s)	P(E,T)(%)
MoO_3	5.65	3.51	$5.04 \cdot 10^{27}$	78.75
MoO_3/CuI	5.85	3.72	$5.22 \cdot 10^{27}$	79.14

In order to go further in the discussion, we have exploited more the prepared PHJ-OPVs by examining their evolution over time depending on the HTL used. Following the protocol proposed in the reference [46], the procedure used to study the ageing process of our OPVs corresponds to the intermediate level labeled ‘‘Level 2’’. The operational life times have been measured under AM1.5, in air and at room temperature, between every measure OPVs were stored in air and in the light of day, the OPVs being in open circuit conditions. The variation with time of the normalized PCE for OPVs stored in ambient atmosphere show that the rate of the PCE decrease depends on the nature of the HTL. Actually, the variation with time of OPVs efficiency with MoO_3 or MoO_3/CuI(1.5 nm) as HTL is similar. In order to understand this behavior, we have also studied the time response of the cell prepared with CuI alone. The results have shown that the efficiency degradation with CuI as HTL is faster. It means that the presence of MoO_3 in the HTL allows improving the OPVs lifetime. For instance, the operational lifetime $T\eta_0/2$, which is defined as the time at which the initial performances have been divided by two [47] of the OPV with MoO_3 is 32 h, while it is 21 h with CuI(1.5 nm) the obtained results are in the Figure S3 in the supporting information. In fact, the transfers of charges at electrodes are sensitive to degradation phenomena. Since the degradation effect is faster when CuI is used alone as ABL, while it is not when CuI is separated from the ITO by a thin MoO_3 film it can be deduced from this observation that there is some degradation of the ITO/CuI interface. This degradation can result from some progressive reaction between ITO and CuI. which is prevented by the insertion of a MoO_3 layer between ITO and CuI.

3. Conclusion

In this study, we have investigated the effect of different HTLs : MoO_3(4nm), MoO_3/CuI and CuI on the performances of the PHJ-OPVs based on the α-6T/C_{60} couple. The results have demonstrated that the use of MoO_3/CuI (1.5 nm) leads to an important enhancements in the PV performances of the α-6T/C_{60} OPV system. By comparing with the cell with single HTL MoO_3 or CuI, we have obtained significant increase in the Voc, J_{sc} and FF from 0.3 V, 4.33 mA/cm2 and 55% in the case of MoO_3 HTL to 0.46 V, 6.19 mA/cm2 and 61% in the case of MoO_3/CuI(1.5nm) respectively which gives rise in the PCE from

0.74% to 1.74%. Moreover, the optimization of the α-6T thickness and its deposition speed rate increases the PCE to 1.77%. A deeper explanation of these results has been done through the study of the structural and the morphological characterization of α-6T layers deposited on HTL with and without CuI. The X-Ray diffraction study shows that CuI has a spectacular effect on the growth of α-6T layers. The layers changed from the amorphous phase to the monoclinic crystalline phase of α-6T, with a lying down molecular orientation, this leads to an important increase of the absorption. Moreover, the 'holes only' measurement revealed an increase in the holes mobility of the α-6T layer by the use of MoO_3/CuI(1.5 nm) HTL. At the end we have exploited more the prepared PHJ-OPVs by examining their evolution over time depending on the HTL used, the results revealed that the MoO_3/CuI(1.5 nm) leads to an increase in the life time of the device by comparing with the other HTLs (MoO_3 and CuI). These findings encourage us to study a ternary device based MoO_3/CuI(1.5 nm) HTL and α-6T/ambipolar layer/C_{60} active layers. This may has the potential to lead to a considerable increase in the efficiency.

Acknowledgements

We gratefully acknowledge « le Centre National de la Recherche Scientifique et Technique (CNRST) » (PPR/2015/9 –Ministère Marocain), le Partenariat Hubert Curien (PHC) franco-marocain TOUBKAL project, under contract No. 41406ZC and the Egypt-France scientific and technological cooperation program " IMHOTEP " under contract No. 44045UF for supporting this work.

References

[1] P.Rand Barry and P.Henning Richter, *Organic Solar Cells Fundamentals, Devices, and Upscaling*.Chapter 1 : Solution-Processed Donors, page 22. 2014.International Standard Book Number-13: 978-981-4463-66-9.

[2] J.C. Bernède, " Organic Photovoltaic Cells: History, Principle and Techniques." *Journal of the Chilean Chemical Society* 53(3):1549–64.(2008), http://dx.doi.org/10.4067/S0717 97072008000300001

[3] L. Cattin, Z. El Jouad, L. Arzel, G. Neculqueo, M. Morsli, F. Martinez, M. Addou, J.C. Bernède "Comparison of performances of three active layers cascade OPVCs with those obtained from corresponding bi-layers," *Sol. Energy*, vol. 171, no. July, pp. 621–628, 2018.DOI :https://doi.org/10.1016/j.solener.2018.07.008

[4] O. Ievgen, K. Wlodzimierz, D.S. Francis, "Evolution of molecular design of porphyrin chromophores for photovoltaic materials of superior light-to- electricity conversion efficiency", Solar RRL 1 (2017) 1600002, https://doi.org/ 10.1002/solr.201600002

[5] X. lu and Q. Z. Xiaobing Fan, Jianhong Gao, Wei Wang, Shengqiang Xiao, Chun Zhan, "Ladder-Type Nonacyclic Arene Bis(thieno[3,2-b]thieno)cyclopentafluorene as a Promising Building Block for Non-Fullerene Acceptors," *Chem. - An Asian J.*, vol. 14, no. 10, pp. 1814–1822, 2019.

[6] H. Sun, X. Song, J. Xie, P. Sun, P. Gu, C. Liu, F. Chen, Q. Zhang, Z-K. Chen and W. Huang., "PDI Derivative through Fine-Tuning the Molecular Structure for Fullerene-Free Organic Solar Cells," *ACS Appl. Mater. Interfaces*, vol. 9, no. 35, pp. 29924–29931, 2017. DOI : 10.1021/acsami.7b08282

[7] Z. Zhang and Y. Lin, "Organic Semiconductors for Vacuum-Deposited Planar Heterojunction Solar Cells," *ACS Omega*, pp. 0–5, 2020. DOI : 10.1021/acsomega.0c03868

[8] M. Levichkova, D. Wynands, A. A. Levin, K. Walzer, D. Hildebrandt, M. Pfeiffer, V. Janonis, M. Pranaitis, V. Kazukauskas, K. Leo, M. Riede. "Dicyanovinyl sexithiophene as donor material in organic planar heterojunction solar cells : Morphological , optical , and electrical properties," *Org. Electron.*, vol. 12, pp. 2243–2252, 2011.DOI : 10.1016/j.orgel.2011.09.022

[9] J.C. Wittmann, C. Straupé, S. Meyer, B.Lotz, P.Lang, G.Horowitz, F.Garnier, "Sexithiophene thin films epitaxially oriented on polytetrafluoroethylene substrates: structure and morphology," *Thin Solid Films*, vol. 333, no. 1–2, pp. 272–277, 1998. DOI : 10.1016/S0040-6090(98)00897-9

[10] H. E. Katz, A. Dodabalapur, Z. Bao, "Oligo- and Polythiophene Field Effect Transistors," Chap 9 in: *Handbook of Oligo- and Polythiophenes*, D. D. Fichou, Ed., Wiley-VCH Verlag GmbH, 1999.

[11] S. Nagamatsu, K. Kaneto, R. Azumi, M. Matsumoto, Y. Yoshida, and K. Yase, "Correlation of the Number of Thiophene Units with Structural Order and Carrier Mobility in Unsubstituted Even- and Odd-Numbered α-Oligothiophene Films," *J. Phys. Chem. B*, vol. 109, no. 19, pp. 9374–9378, 2005.

[12] J-H. Choi, M. E.El-Khouly, T. Kim, Y-Su Kim, U-C. Yoon, S. Fukuzumi and K. Kim, "Solution-processed bulk heterojunction solar cells with silyl end-capped sexithiophene," *Int. J. Photoenergy*, vol. 2013, 2013. DOI :10.1155/2013/843615

[13] K. Cnops, B-P. Rand, D. Cheyns, B. Verreet, M. A. Empl and P. Heremans, "8.4% Efficient Fullerene-Free Organic Solar Cells Exploiting Long-Range Exciton Energy Transfer," *Nat. Commun.*, vol. 5, pp. 1–6, 2014. DOI :10.1038/ncomms4406

[14] J-C. Bernède, L. Cattin, M. Makha, V. Jeux, L. Philippe, J. Roncali, V. Froger and M. Addou., "MoO_3CuI hybrid buffer layer for the optimization of organic solar cells based on a donor – acceptor triphenylamine," *Sol. Energy Mater. Sol. Cells*, vol. 110, pp. 107–114, 2013. DOI : 10.1016/j.solmat.2012.12.003

[15] N. R. Armstrong, C. Carter, C. Donley, A. Simmonds, P. Lee, M. Brumbach, B. Kippelen, B. Domercq, S. Yoo, "Interface modification of ITO thin films: Organic photovoltaic cells," *Thin Solid Films*, vol. 445, no. 2, pp. 342–352, 2003. DOI : 10.1016/j.tsf.2003.08.067

[16] A. Opitz, J. Wagner, W. Brutting, I. Salzmann, N. Koch, J. Manara, J. Pflaum, A. Hinderhofer and F. Schreiber, "Charge separation at molecular donor-acceptor interfaces: Correlation between morphology and solar cell performance," *IEEE J. Sel. Top. Quantum Electron.*, vol. 16, no. 6, pp. 1707–1717, 2010. DOI : 10.1109/JSTQE.2010.2048096

[17] C. Lorch, R. Banerjee, J. Dieterle, A. Hinderhofer, A. Gerlach, J. Drnec and F. Schreiber, "Templating Effects of α-Sexithiophene in Donor-Acceptor Organic Thin Films," *J. Phys. Chem. C*, vol. 119, no. 40, pp. 23211–23220, 2015.

[18] A. Hinderhofer, A. Gerlach, K. Broch, T. Hosokai, K. Yonezawa, K. Kato, S. Kera, N. Ueno and F. Schreiber, "Geometric and electronic structure of templated C_{60} on diindenoperylene thin films," *J. Phys. Chem. C*, vol. 117, no. 2, pp. 1053–1058, 2013.DOI.org/10.1021/jp3106056 |

[19] J. C. Bernède, L. Cattin, M. Morsli, S. R. B. Kanth, S. Patil, and N. Stephant, "Improvement of the efficiency of organic solar cells using the terthiophene-pyran-malononitrile (T3PM) as electron donor, through the use of a MoO3/CuI anode buffer layer," *Energy Procedia*, vol. 31, pp. 81–88, 2012.

[20] L. Pithan, C. Cochi, H. Zschiesche, C. Weber, A. Zykov, S. Bommel, S. J. Leake, P. Schafer, C. Draxl and S. Kowarik, "Light Controls Polymorphism in Thin Films of Sexithiophene," *J. Crystal Growth and Design*, pp. 1–6, 2015. DOI : 10.1021/cg501734w

[21] T. Taima, Md. Shahiduzzaman, T. Ishizeki, K. Yamamoto, M. Karakawa, T. Kuwabara and K. Takahashi, "Sexithiophene-Based Photovoltaic Cells with High Light Absorption Coefficient via Crystalline Polymorph Control," *J. Phys. Chem. C*, vol. 121, no. 36, pp. 19699–19704, 2017. DOI : 10.1021/acs.jpcc.7b07953

[22] K. Yamamoto, Md. Shahiduzzaman, A. Yamada, T.Takaya, T. Chikamatsu, T. Koganezawa, M. Karakawa, T. Kuwabara, K. Takahachi, T. Taima "Molecular orientation control of semiconducting molecules using a metal layer formed by wet processing," *Org. Electron.*, vol. 63, no. May, pp. 47–51, 2018, DOI : https://doi.org/10.1016/j.orgel.2018.09.008

[23] Md. Shahiduzzaman, T. Horikawa, T. Hirayama, M. Nakano, M. Karakawa, K. Takahashi, J-M. Nunzi and T. Taima, "Switchable Crystal Phase and Orientation of Evaporated Zinc Phthalocyanine Films for Efficient Organic Photovoltaics," *J. Phys. Chem. C*, vol. 124, no. 39, pp. 21338–21345, 2020. DOI : 10.1021/acs.jpcc.0c07010

[24] L. Cattin, J.C. Bernède, Y. Lare, S. Dados-Seignon, N. Stephant, M. Morsli, P.P. Zamora, F.R. Diaz and M.A. del Valle "Improved performance of organic solar cells by growth optimization of MoO3/CuI double-anode buffer," *Phys. Status Solidi Appl. Mater. Sci.*, vol. 210, no. 4, pp. 802–808, 2013. DOI : 10.1002/pssa.201228665

[25] B-P. Rand, D. Cheyns, K. Vasseur, N.C. Giebink, S. Mothy, Y. Yi, V. Coropceanu, D. Beljonne, J. Cormil, J-L. Brédas and J .Genoe, "The impact of molecular orientation on the photovoltaic properties of a phthalocyanine/fullerene heterojunction," *Adv. Funct. Mater.*, vol. 22, no. 14, pp. 2987–2995, 2012. DOI : 10.1002/adfm.201200512.

[26] H-J. Kim, H-S. Shim, J-W. Kim, H-H. Lee and J-J. Kim, "CuI interlayers in lead phthalocyanine thin films enhance near-infrared light absorption," *AIP Appl. Phys. Lett.*, vol. 263303, no. 2012, pp. 2010–2014, 2013. DOI : 10.1063/1.4730604

[27] H. Ulrich, C. Lorch, A. Hinderhofer, A. Gerlach, M. Gruber, J. Kraus, B. Sykora, S. Grob, T. Linderl, A. Wilke, A. Opitz, R. Hansson, A-S. Anselmo, Y. Ozawa, Y. Nakayama, H. Ishii, N. Koch, E. Moons, F. Schreiber, and W. Brutting, "Voc from a morphology point of view: The influence of molecular orientation on the open circuit voltage of organic planar heterojunction solar cells," *J. Phys. Chem. C*, vol. 118, no. 46, pp. 26462–26470, 2014. DOI : 10.1021/jp506180k.

[28] J. Sakai, T. Taima, and K. Saito, "Efficient oligothiophene:fullerene bulk heterojunction organic photovoltaic cells," *Org. Electron.*, vol. 9, no. 5, pp. 582–590, 2008. DOI : 10.1016/j.orgel.2008.03.008

[29] B. Johnev, M. Vogel, K.Fostiropoulos, B. Mertesacker, M. Rusu, M.-C. Lux-Steiner, A. Weidinger, "Monolayer passivation of the transparent electrode in organic solar cells," *Thin Solid Films*, vol. 488, no. 1–2, pp. 270–273, 2005. DOI : 10.1016/j.tsf.2005.04.058

[30] L. Cattin, Z. El Jouad, L. Arzel, G. Neculqueo, M. Morsli, F. Martinez, M. Addou, J.C. Bernède, "Comparison of performances of three active layers cascade OPVCs with those obtained from corresponding bi-layers," *Sol. Energy*, vol. 171, no. July, pp. 621–628, 2018. DOI : 10.1016/j.solener.2018.07.008

[31] J. C. Bernède, Y. Berredjem, L. Cattin, and M. Morsli, "Improvement of organic solar cell performances using a zinc oxide anode coated by an ultrathin metallic layer," *Appl. Phys. Lett.*, vol. 92, no. 8, pp. 37–40, 2008. DOI : 10.1063/1.2888176

[32] A.S. Yapi, L. Toumi, Y. Lare. G.M. Soto, L. Cattin, K.Toubal, A. Djafri, M. Morsli, A. Khelil, M.A. Del Valle, and J.-C. Bernède, "On the influence of the exciton-blocking layer on the organic multilayer cells properties," *EPJ Appl. Phys.*, vol. 50, no. 3, pp. 30403-p1-30403-p8, 2010. DOI : 10.1051/epjap/2010062

[33] J-C. Bernède, L. Cattin, M. Makha, V. Jeux, P. Leriche, J. Roncali, V. Froger, M. Morsli, "MoO_3/CuI hybrid buffer layer for the optimization of organic solar cells based on a donor–acceptor triphenylamine," *Sol. Energy Mater. Sol. Cells*, pp. 107–114, 2013. DOI : http://dx.doi.org/10.1016/j.solmat.2012.12.003

[34] Y. Zang, J. Yu, J. Huang, R. Jiang, and G. Huang, "Fill factor of planar heterojunction organic solar cells with varied donor materials," *J. Phys. D. Appl. Phys.*, vol. 45, no. 17, 2012. DOI : 10.1088/0022-3727/45/17/175101

[35] P.A. Lane, X. Wei, Z.V. Vardeny, J. Poplawski, E. Ehrenfreud, M. Ibrahim, A.J. Frank, "Absorption spectroscopy of charged excitations in α-sexithiophene: Evidence for charge conjugation symmetry breaking," *Chem. Phys.*, vol. 210, no. 1-2 SPEC. ISS., pp. 229–234, 1996. DOI : 10.1016/0301-0104(96)00075-4

[36] T. Mizokuro, C. Heck, and N. Tanigaki, "Orientation of α-Sexithiophene on friction-transferred polythiophene film," *J. Phys. Chem. B*, vol. 116, no. 1, pp. 189–193, 2012. DOI : 10.1021/jp207487z

[37] J.-C. Blakesley, A. F. Castro, W. Kylberg, George F.A. Dibb, C. Arantes, R. Valaski, M. Cremona, J- S. Kim, "Towards reliable charge-mobility benchmark measurements for organic semiconductors," *Org. Electron.*, vol. 15, no. 6, pp. 1263–1272, 2014. DOI : http://dx.doi.org/10.1016/j.orgel.2014.02.008

[38] M. Makha, L. Cattin, S. Dabos-Seignon, E. Arca, J. Velez, N. Stephant, M. Morsli, M. Addou, J-C. Bernède, "Study of CuI thin films properties for application as anode buffer layer in organic solar cells," *Indian J. Pure Appl. Phys.*, vol. 51, no. 8, pp. 569–582, 2013.

[39] M. Grundman, F-L. Chein, M. Lorenz, T. Bontgen, J. Lenzner and H. V. Wenckstern "Cuprous iodide - A p-type transparent semiconductor: History and novel applications," *Phys. Status Solidi Appl. Mater. Sci.*, vol. 210, no. 9, pp. 1671–1703, 2013. DOI : https://doi.org/10.1002/pssa.201329349.

[40] T. Mizokuro, K. Takeuchi, C. Heck, and H. Aota, "Orientation management of a -sexithiophene layer for the application in organic photovoltaic devices," *Org. Electron.*, vol. 13, no. 12, pp. 3130–3137, 2012. DOI : 10.1016/j.orgel.2012.09.017

[41] N. K. Elumalai and A. Uddin, "Open circuit voltage of organic solar cells: An in-depth review," *Energy Environ. Sci.*, vol. 9, no. 2, pp. 391–410, 2016. https://doi.org/10.1039/C5EE02871J

[42] B. Ebenhoch, S. A.J. Thomson, K. Genevicius, G. Juška, Ifor D.W. Samuel, "Charge carrier mobility of the organic photovoltaic materials PTB7 and PC71BM and its influence on device performance," *Org. Electron.*, vol. 22, pp. 62–68, 2015, DOI : 10.1016/j.orgel.2015.03.013

[43] S. Duhm, , G. Heime, I. Salzmann, H. Glowatzki, Robert L. Johnson , A. Vollmer, J. P. Rabel and N. Koch "Orientation-dependent ionization energies and interface dipoles in ordered molecular assemblies", *Nature Materials. vol. 7, pp.* 326-332, 2008, DOI : 10.1038/nmat2119.

[44] Q. An, F. Zhang, Q. Sun, M. Zhang, J. Zhang, W. Tang, X. Yin, Z. Deng, "Efficient organic ternary solar cells with the third component as energy acceptor," *Nano Energy*, vol. 26, pp. 180–191, 2016. DOI : http://dx.doi.org/10.1016/j.nanoen.2016.05.018

[45] M.B. Siad, Z. El Jouad, A. Khelil, A. Mohammed Krarroubi, S. Morsli, G. Neculqueo, M. Addou, J.C. Bernède and L. Cattin, "Comparison of Performances of Organic Photovoltaic Cells Using SubPc as Central Ambipolar Layer in Ternary Structures and as Electron Acceptor in Binary Structures," *Surf. Rev. Lett.*, vol. 1950184, no. December, pp. 1–10, 2019. DOI : 10.1142/S0218625X19501841

[46] M.O. Reesea, S.A. Gevorgyan, M. Jørgensen, E. Bundgaard, S.R. Kurtz , D.S. Ginley, D.C. Olson, M.T. Lloyd, P. Morvillo, A. Elschner , O. Haillant , T.R.Currier, V. Shrotriya, M. Hermenau, M. Riede, K.R. Kirov, G. Trimmel, F.C. Krebs, " Consensus stability testing protocols for organic photovoltaic materials and devices" Vol 95, Issue 5, May 2011, Pages 1253-1267, https://doi.org/10.1016/j.solmat.2011.01.036

[47] G. Dennler, C. Lungenschmied, H. Neugebauer, N.S. Sariciftci, M. Latrèche, G. Czeremuszkin, M.R. Wertheimer "A new encapsulation solution for flexible organic solar cells" Thin Solid Films 511–512 (2006) 349 – 353 https://doi.org/10.1016/j.tsf.2005.12.091

[48] M. Kohlstädt, M. Grein, P. Reinecke, T. Kroyer, B. Zimmermann, U. Würfel "Inverted ITO- and PEDOT:PSS-free polymer solar cells with high power conversion efficiency" Solar Energy Materials & Solar Cells 117 (2013) 98–102, https://doi.org/10.1016/j.solmat.2013.05.023

[49] M. Makha, L. Cattin, S. Ouro Djobo, N. Stephant, N. Langlois, B. Angleraud, M. Morsli, M. Addou, and J-C. Bernède "Effect of the nature of the anode buffer layer - MoO_3, CuI or MoO_3/CuI - On the performances of organic solar cells based on oligothiophene thin films deposited by sublimation", https://doi.org/10.1051/epjap/2012120372.

Table 1: PV parameters of the both devices Table 1. Variation of the PV parameters of PHJ-OPVs with the HTL used : MoO_3 or MoO_3/CuI(1.5 nm), MoO_3/CuI(3 nm) and CuI(1.5 nm) MoO_3 or MoO_3/CuI

HTL	α-6T thickness (nm)	CuI thickness (nm)	V_{oc} (V)	J_{sc} (mA/cm^2)	FF (%)	PCE (%)
MoO_3	20	----	0.31 ± 0.04	4.33 ± 0.50	55 ± 3	0.74 ± 0.30
MoO_3/CuI	**20**	**1.5**	**0.46 ± 0.03**	**6.19 ± 0.40**	**61 ± 3**	**1.74 ± 0.25**
MoO_3/CuI	20	3	0.41 ± 0.05	5.99 ± 0.50	54 ± 4	1.33 ± 0.35
CuI	20	1.5	0.41 ±0 .05	5.80 ± 0.60	44 ± 5	1.06 ± 0.40

HTL	α-6T thickness (nm)	V_{oc} (V)	J_{sc} (mA/cm^2)	FF (%)	PCE (%)
MoO_3/CuI(1.5 nm)	18	0.43 ± 0.04	3.40 ± 0.50	63 ± 4	0.93 ± 0.30
	20	0.46 ± 0.03	6.19 ± 0.40	61 ± 3	1.74 ± 0.25
	22	**0.50 ± 0.03**	**6.10 ± 0.35**	**58 ± 4**	**1.77 ± 0.25**
	24	0.46 ± 0.03	5.44 ± 0.45	55 ± 5	1.38 ± 0.30
MoO_3	**22**	**0.31± 0.04**	**4.25 ± 0.5**	**56 ± 3**	**0.74 ± 0.30**

Table 2. Variation of the PV parameters of the α-6T/C_{60} OPVs with α-6T thickness and the PV parameters of the cell prepared with the optimum α-6T thickness using MoO_3 HTL alone.

Table 3

Table 3. Different physical parameters estimated from the J_{ph} vs. V_{eff} curves for the cells with and without CuI

	$J_{sat}(mA/cm^2)$	$J_{ph}(mA/cm^2)$	G_{max} (Photon/m^3.s)	P(E,T)(%)
MoO3	5.65	3.51	$5.04 \cdot 10^{27}$	78.75
MoO3/CuI	5.85	3.72	$5.22 \cdot 10^{27}$	79.14

Figure 1. The stacked device architecture (a), the structures of the applied actives materials (b) and a schematics representation of the energy diagram (c)

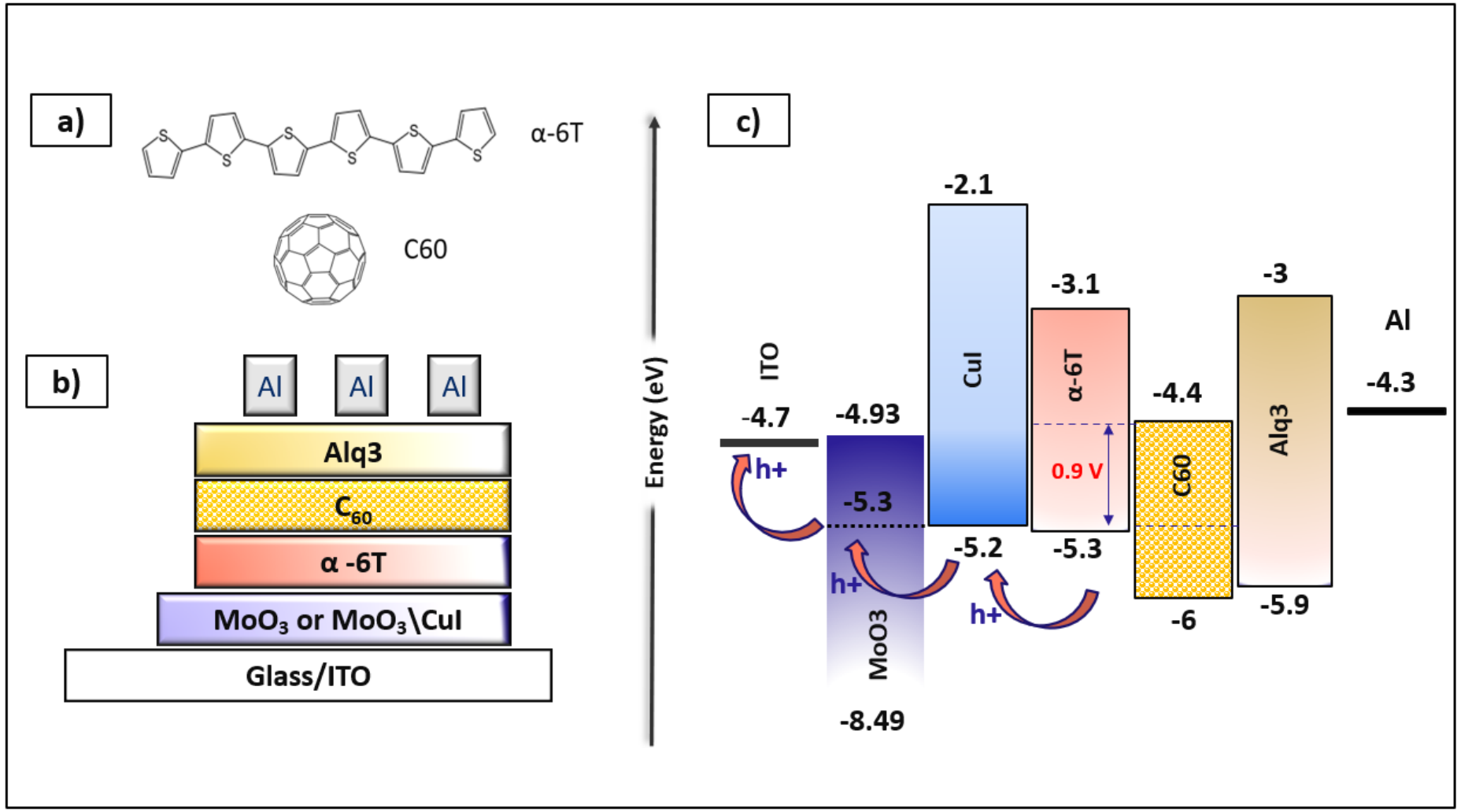

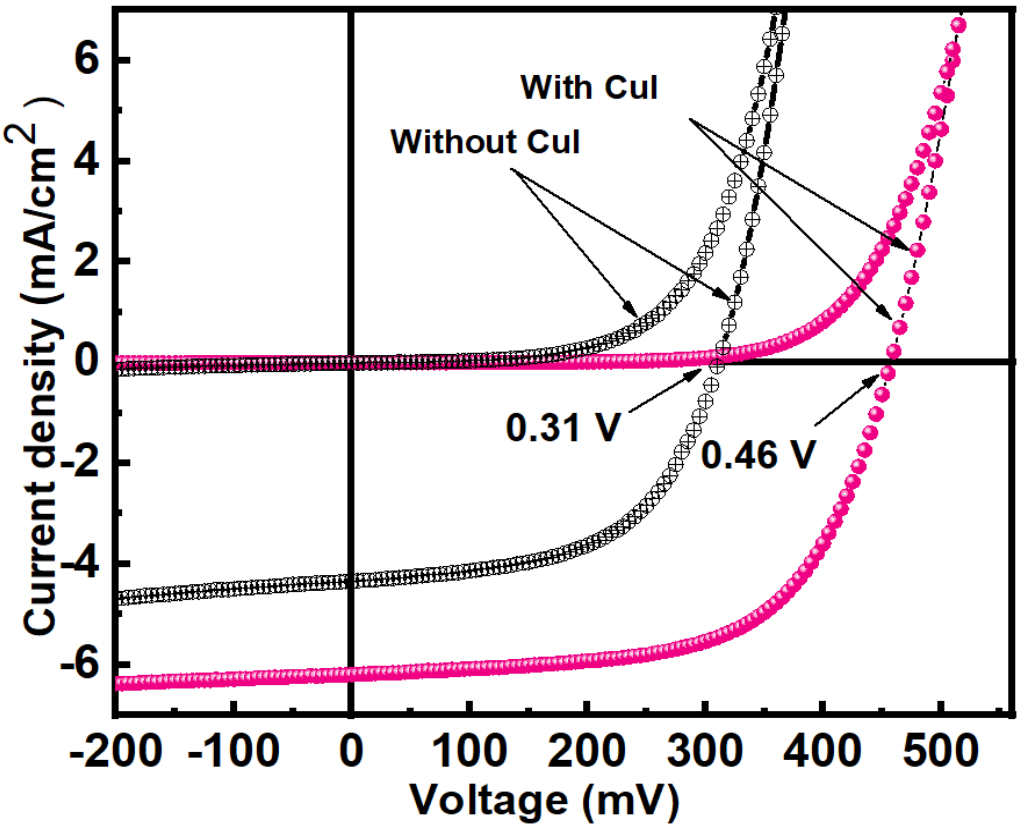

Fig. 2. Electrical OPV devices characteristics with MoO_3/CuI (1.5 nm) (●) and MoO_3 (⊕) HTLs

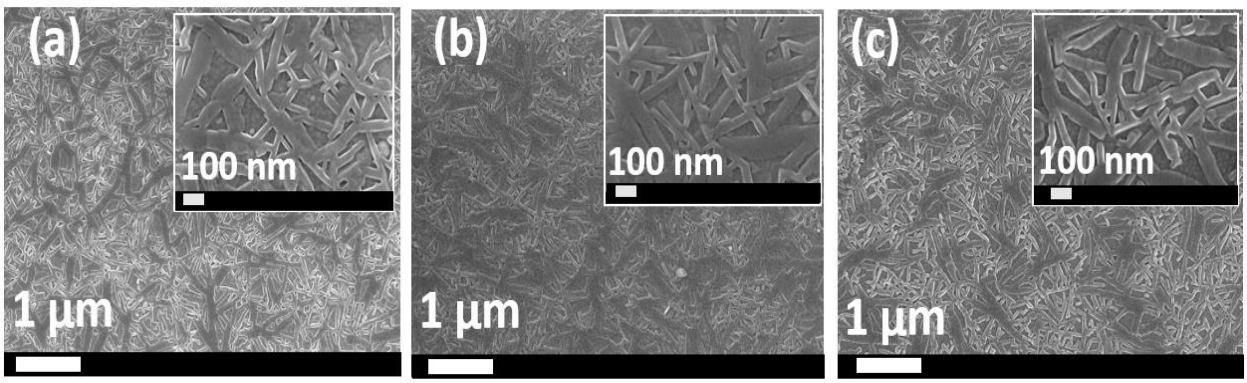

Fig. 3. SEM images of the α-6T deposited with different speed rates (a) low speed (0.01-0.03 nm/s), (b) medium speed rate (0.04 – 0.06 nm/s) and (c) fast speed rate (0.06-0.08 nm/s). Inset. larger magnification.

Figure 4. Optical density spectrums of α-6T films deposited with low speed (0.01-0.03 nm/s), medium speed rate (0.04 – 0.06 nm/s) and fast speed rate (0.06-0.08 nm/s)

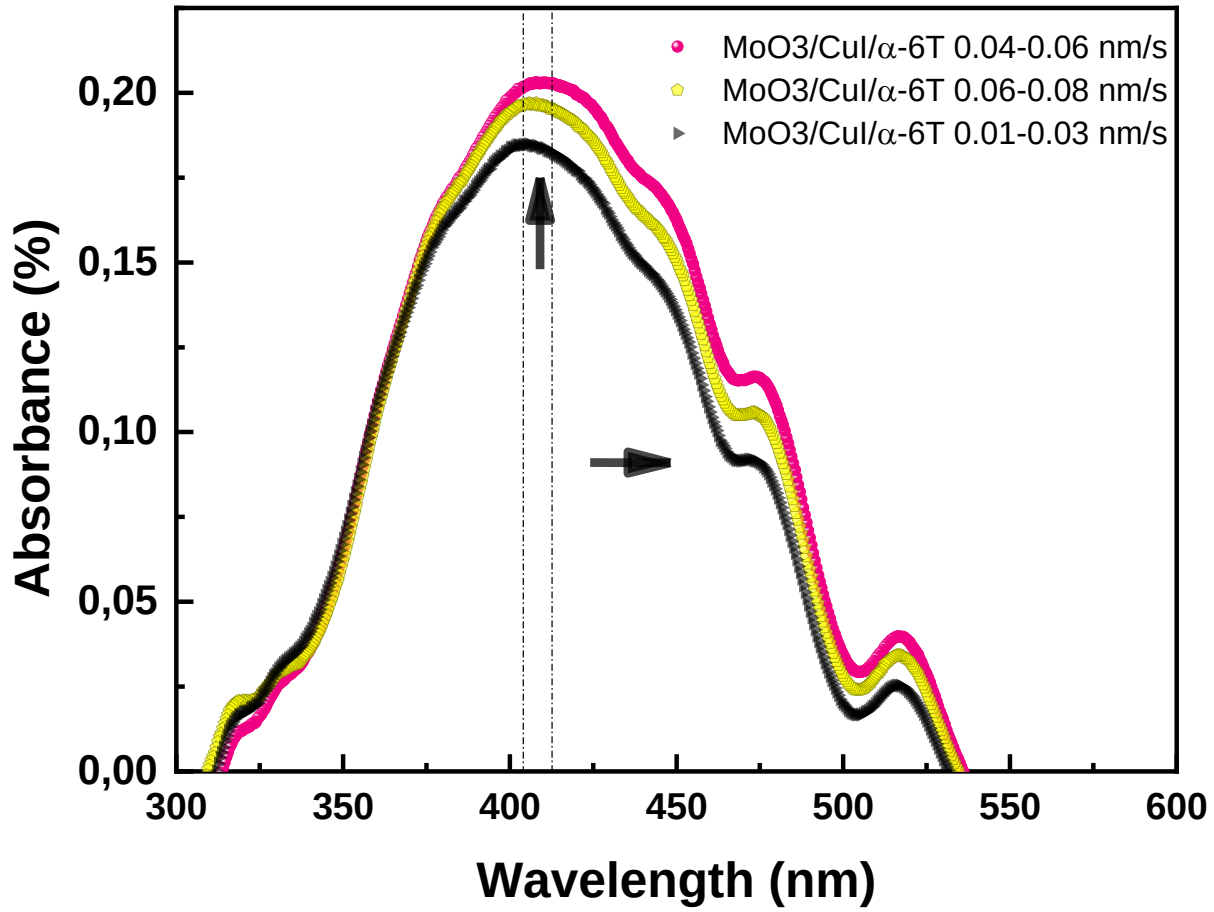

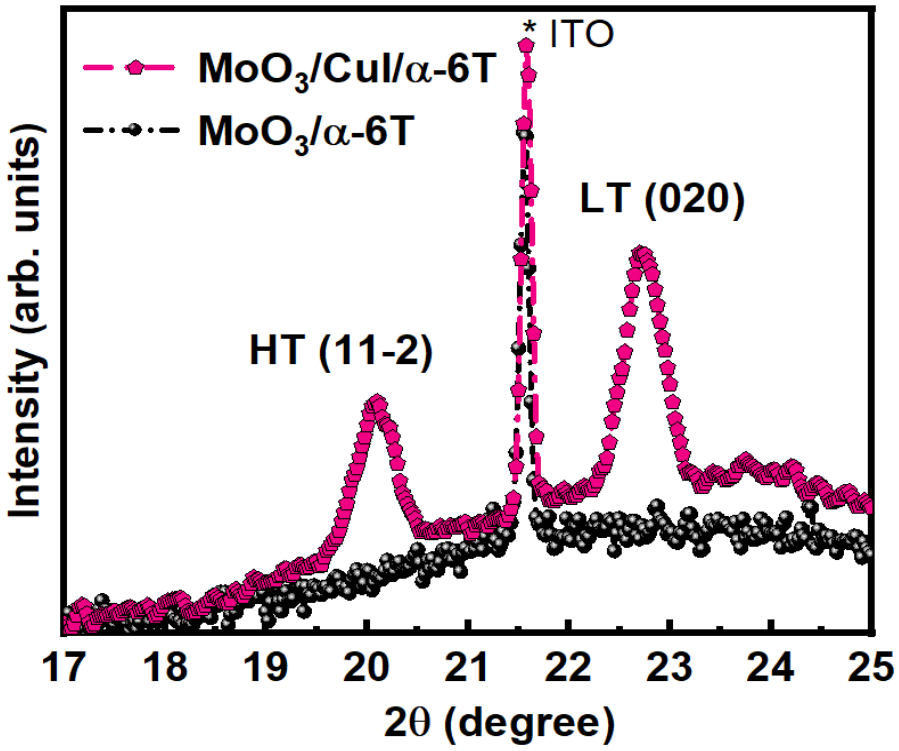

Fig. 5. XRD patterns of α-6T films deposited on ITO/MoO_3 and ITO/MoO_3/CuI(1.5 nm)

Figure 6. Optical density spectrums of α-6T films deposited on ITO/MoO_3 and ITO/MoO_3/CuI

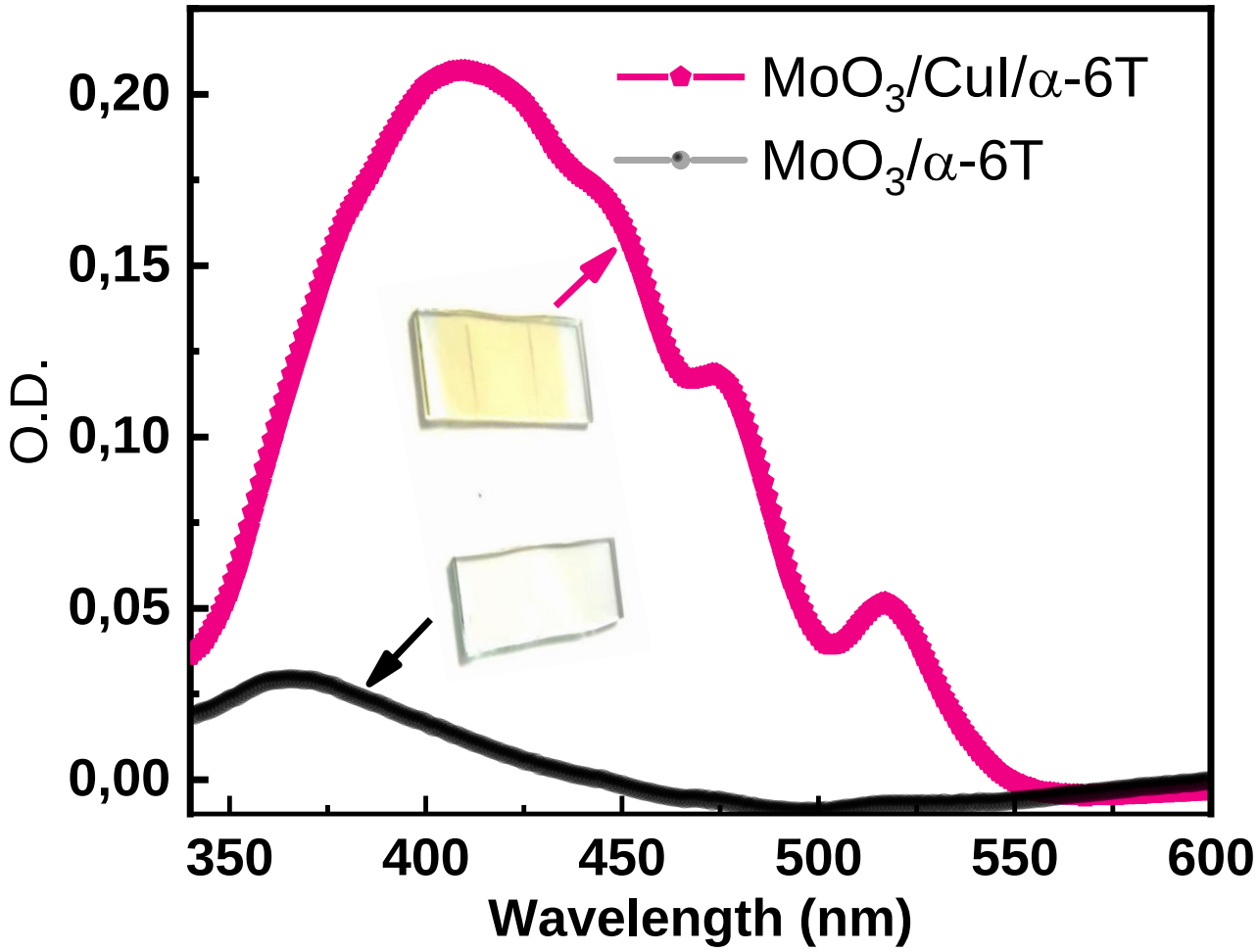

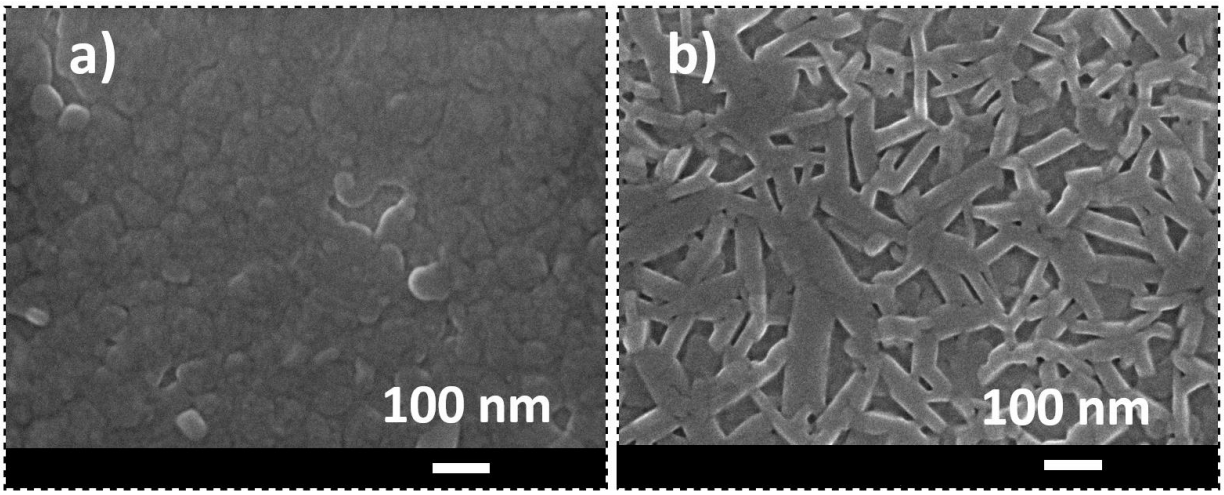

Fig.7. SEM images of the α-6T deposited on MoO_3 (a) and on MoO_3/CuI(1.5 nm) (b)

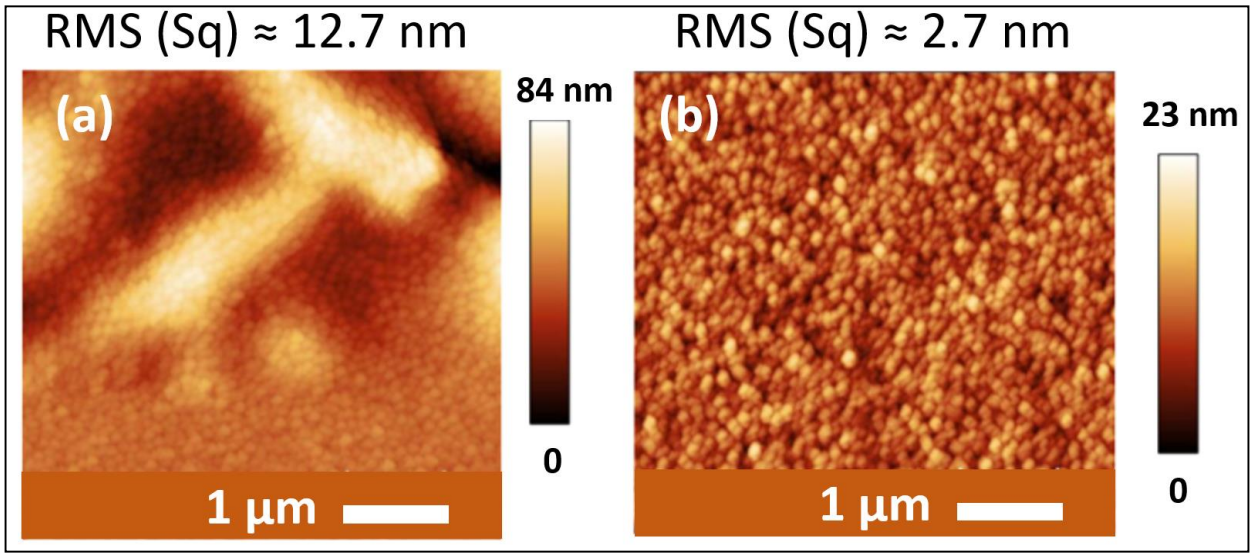

Fig.8. AFM images of the α-6T deposited on MoO_3 (a) and on MoO_3/CuI(1.5 nm) (b)

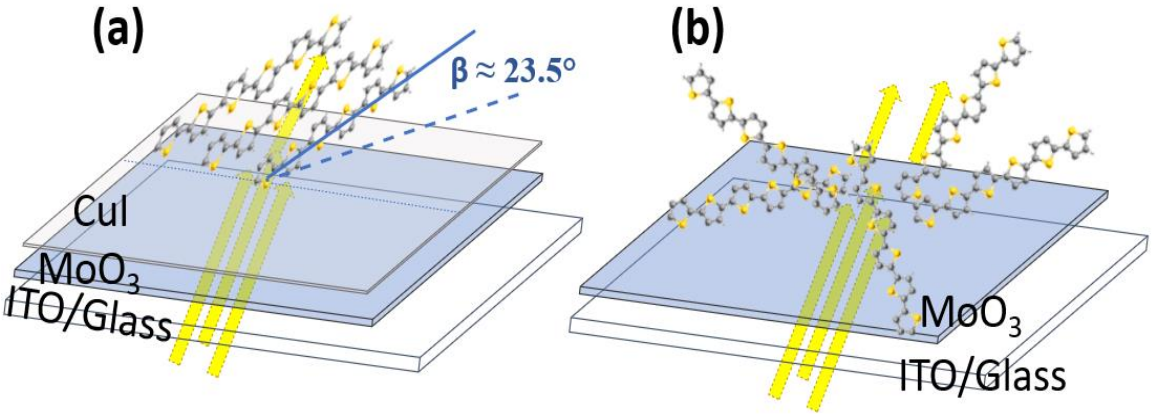

Fig.9. Schematic illustration of the absorption dependence of the α-6T in the case of ordered structure with the laying down molecular orientation (ITO/MoO_3/CuI/α-6T) (a) and the disordered structure (ITO/MoO_3/α-6T) (b)

Figure 10. J_{ph} vs. V_{eff} curves for α-6T/C_{60} PHJ-OSCs devices with the both HTL MoO_3 and MoO_3/CuI HTLs

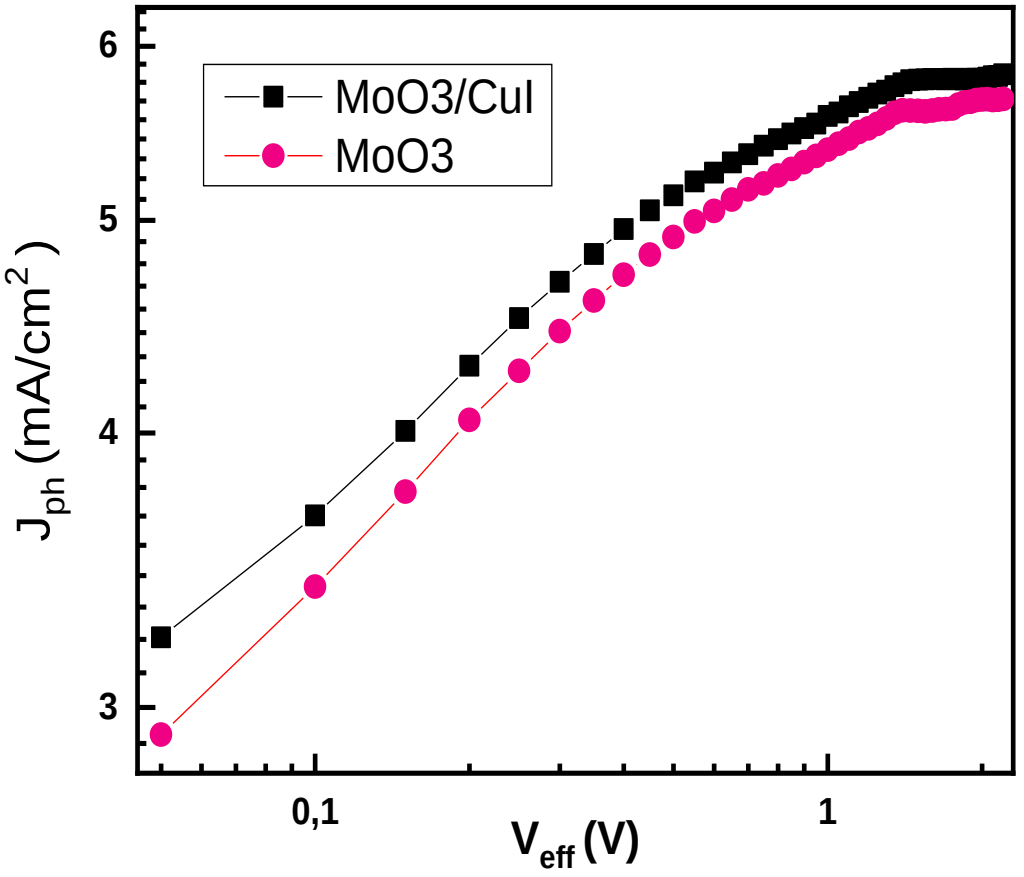

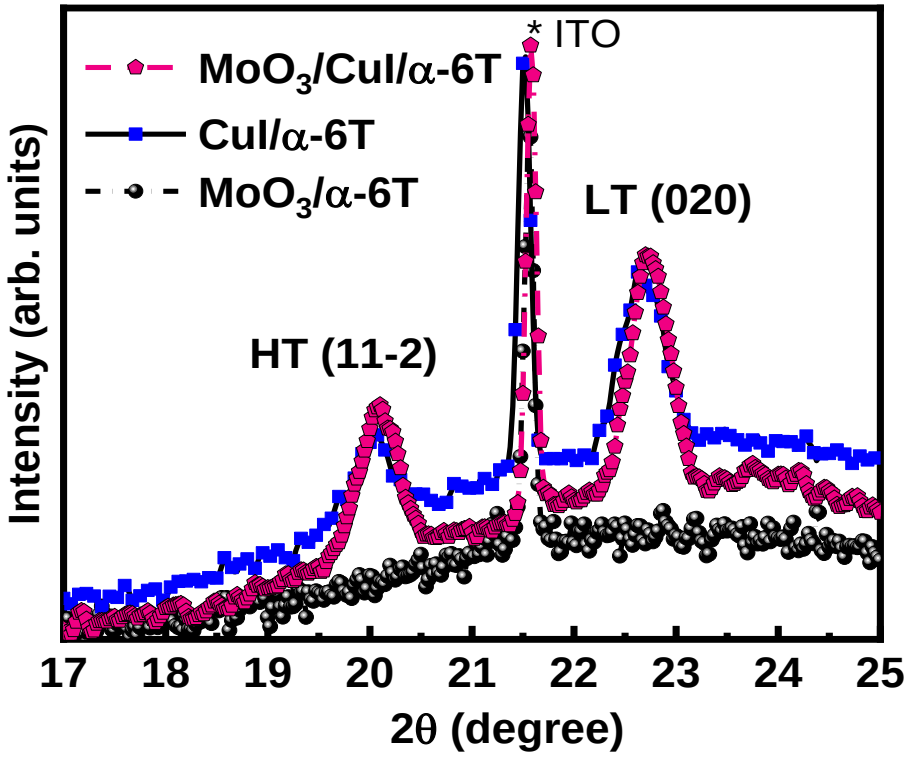

Fig. S1. XRD patterns of α-6T films deposited on ITO/MoO_3 , ITO/CuI and ITO/MoO_3/CuI(1.5 nm)

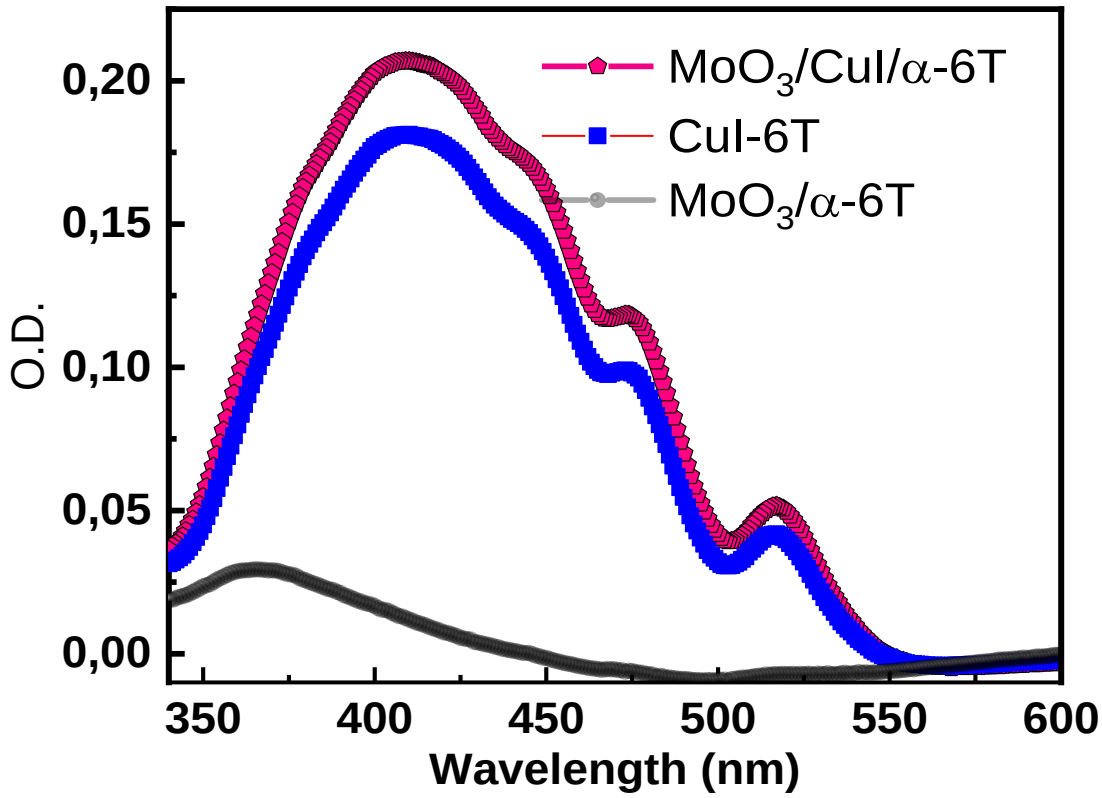

Fig. S2. Optical density spectrums of α-6T films deposited on MoO_3, MoO_3/CuI(1.5 nm) and CuI HTLs

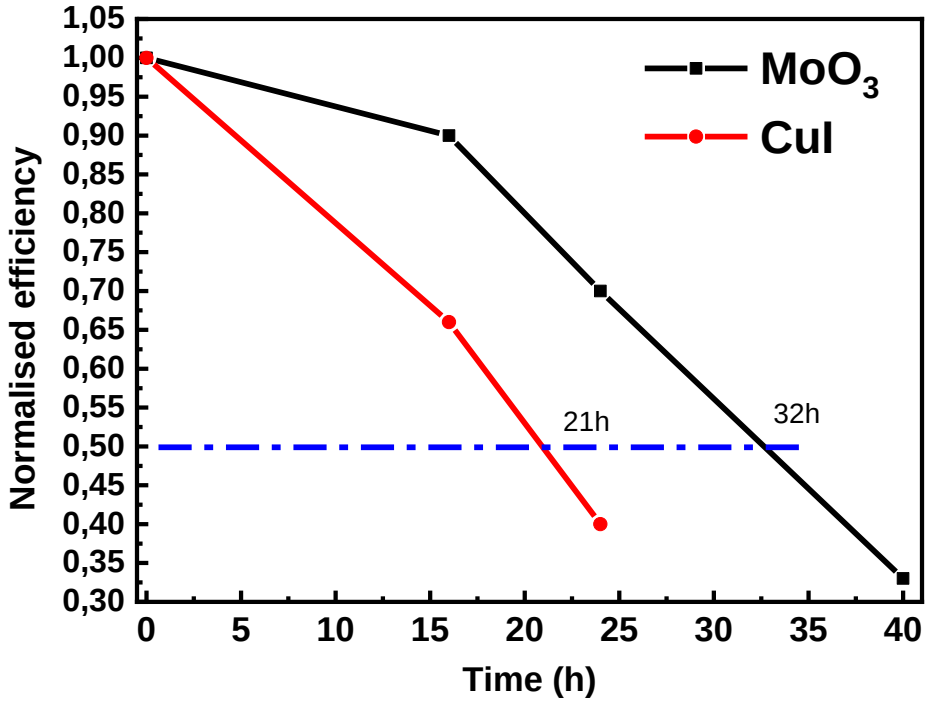

Fig. S3. The variation of the time response of the prepared PHJ-OPVs with the HTL used